Paleosol-based inference of niches for Oligocene and early miocene fossils from the John Day Formation of Oregon

Gregory J. Retallack & Joshua X. Samuels

View supplementary material

Published online: 16 Jun 2020.

Submit your article to this journal

View related articles

View Crossmark data

Check for updates

ARTICLE

PALEOSOL-BASED INFERENCE OF NICHES FOR OLIGOCENE AND EARLY MIOCENE FOSSILS FROM THE JOHN DAY FORMATION OF OREGON

GREGORY J. RETALLACK[*,1] and JOSHUA X. SAMUELS[2]

[1]Department of Earth Sciences, University of Oregon, Eugene, Oregon 97403, U.S.A., gregr@uoregon.edu;
[2]Department of Geosciences, East Tennessee State University, Johnson City, Tennessee 37614, U.S.A., samuelsjx@etsu.edu

ABSTRACT—Over the past decade, we recorded exact locations of in situ fossils and measured calcareous nodules in paleosols of the Oligocene and lower Miocene (Whitneyan–Arikareean) John Day Formation of Oregon. These data enable precise biostratigraphy within an astronomical time scale of Milankovitch obliquity cycles and also provide mean annual precipitation and vegetation for each species. Fossils in paleosols of the John Day Formation alternated between semiarid shrubland and subhumid woodland communities every 41 ka. Land snails 'Polygyra' expansa and Monadenia dubiosa were found in semiarid paleosols, but Vespericola dalli and Monadenia marginicola were found in subhumid paleosols. Cicada burrows (Naktodemasis bowni) were found in semiarid paleosols, whereas dung beetle balls (Pallichnus dakotensis) and earthworm castings (Edaphichnium lumbricatum) were found in subhumid paleosols. Among hypertragulids, Hypertragulus hesperius was found in semiarid paleosols and Nanotragulus planiceps in subhumid paleosols. Among glires, the aplodontiid Haplomys liolophus, geomyids Pleurolicus sulcifrons and several species of Entoptychus, castorid Palaeocastor peninsulatus, and leporid Archaeolagus ennisianus were found in semiarid paleosols. Large ungulates were found primarily in subhumid paleosols, including the agriochoere Agriochoerus antiquus, oreodonts Eporeodon occidentalis and Promerycochoerus superbus, equid Miohippus annectens, and rhinos Diceratherium annectens and Diceratherium armatum. The inferred niches of fossil mammals are consistent with interpretations based on their morphology; taxa with adaptations for life in open, arid habitats, such as high-crowned teeth and semifossorial or cursorial limb structure, were mainly in semiarid paleosols, but taxa with arboreal adaptations were only found in subhumid paleosols.

SUPPLEMENTAL DATA—Supplemental materials are available for this article for free at www.tandfonline.com/UJVP

INTRODUCTION

Ecological niches of extinct species have long been reconstructed in order to understand them as organisms and where and how they lived. Here, we outline novel approaches to niche reconstruction using fossil soils in which the fossils were found, extending preliminary studies on Oligocene fossils of the John Day Formation of Oregon (Retallack et al., 2004). Our approach is distinct from classical functional morphology, for example, linking tooth crown height or occlusal morphology with feeding on different types of plants (Kowalevsky, 1873; Stirton, 1947; Van Valen, 1960; Rosenberger and Kinzey, 1976; Janis, 1988; Janis and Fortelius, 1988; Janis et al., 2002; Damuth and Janis, 2011; Strömberg, 2011; Jardine et al., 2012; Hoffman et al., 2015; Samuels and Hopkins, 2017). Also based on fossil specimens are niches reconstructed from studies of tooth wear (Solounias et al., 1988; Solounias and Semprebon, 2002; Merceron et al., 2009; Mihlbachler et al., 2011), isotopic composition of teeth (Cerling et al., 2004; MacFadden and Higgins, 2004; Zanazzi and Kohn, 2008), and limb ratios (Andrews et al., 1979; Van Valkenburgh, 1985; Garland and Janis, 1993). Another method for Quaternary mammals closer to our approach has been niche modeling by climate inferred from geographic distributions

(Waltari and Guralnick, 2009; Hadley et al., 2009; Nogués-Bravo, 2009; DeSantis et al., 2012; Davis et al., 2014; McGuire and Davis, 2014), and this has been extended to pre-Quaternary mammals (Maguire and Stigall, 2009; DeSantis et al., 2012).

Evidence from paleosols can supplement all of these approaches, because paleosols are themselves evidence of niches (Retallack et al., 2000, 2002), and also provide geochemical, petrographic, and physical proxies for environmental factors (Nordt et al., 2006; Sheldon and Tabor, 2009; Beverly et al., 2018). This paper emphasizes Bk metrics, a variety of measurements of the distribution and size of calcareous nodules in paleosols. For example, the depth to the calcic horizon in a paleosol is related to three productivity-producing variables: (1) mean annual precipitation (Retallack, 2005); (2) tree height (Retallack, 2012); and (3) soil CO_2 at the end of the growing season (Breecker and Retallack, 2014). Soil productivity is the key variable here and is related to both tree height and precipitation (Breecker and Retallack, 2014). The size of nodules in a modern soil is a function of the time over which it formed (Retallack, 2005), and in a paleosol it is thus a guide to ecological successional stage of the community (Retallack, 2004a, 2004b, 2004c, 2005). Calculation of these parameters from paleosols can provide a proxy for the ecology of fossil species contained within (Table 1, S1). Paleosol niches are independent of other proxies, such as functional morphology, isotope geochemistry, or geographic distribution.

Incidentally, the same paleosol Bk metrics measured for niche definition are also useful for biostratigraphy because they show

---

*Corresponding author.
Color versions of one or more of the figures in the article can be found online at www.tandfonline.com/ujvp.

oscillations on Milankovitch time scales (Retallack et al., 2004) and thus allow construction of an astronomical time scale. Astronomical cyclostratigraphy allows meter-level precision needed to determine range confidence intervals (Marshall, 1990, 1997), as opposed to traditional subdivision into thick units, such as Units A–M of the Turtle Cove and Kimberly members of the John Day Formation (Fremd et al., 1994; Albright et al., 2008). A classical technique of collecting fossils in measured sections and then correlating each section is not useful in the John Day Formation, because fossils are so sparse that first appearances are unreliable. Milankovitch obliquity beats of 41 ka, each with at least three paleosols, can be used to correlate stratigraphic level to master sections (Retallack et al., 2004). Thus, outlying fossil occurrences can be linked to a master astronomical cyclostratigraphy. Such biostratigraphic refinement is a novel secondary objective of our study of Oligocene fossils of the John Day Formation.

A limitation of our approach is that it requires expertise in paleopedology and newly collected specimens, because it hinges on determination of (1) whether the fossil is in situ; (2) exactly where in the paleosol it was found; and (3) field measurement or sampling of critical features in the paleosol. This can be done after collection for those rare cases of controlled excavations of fossils in paleosols (Retallack, 1991; Retallack et al., 2002), but unfortunately the vast majority of material previously collected from the John Day Formation is not useful for our purposes. Thus, we have collected hundreds of new fossils and accessioned them into collections of the John Day Fossil Beds National Monument and the Museum of Natural and Cultural History of the University of Oregon, which already had thousands of other specimens from these general localities. This new collection of 504 specimens is inadequate for confident inferences for rare species but can provide revealing data on ecological niches and biostratigraphic resolution of common species of fossil animals.

Institutional Abbreviations—**JODA**, Thomas Condon Paleontology Center, John Day Fossil Beds National Monument, Kimberly, Oregon, U.S.A.; **UOMNH**, Condon Collection of the Museum of Natural and Cultural History of the University of Oregon, Eugene, Oregon, U.S.A.

MATERIALS AND METHODS

Geological Setting

The Turtle Cove, Kimberly, Haystack Valley, Balm Creek, and Johnson Canyon members of the John Day Formation have long been known for fossil mammals (Merriam and Sinclair, 1906; Albright et al., 2008) and are especially well exposed in the John Day Valley between Spray and Picture Gorge (Fig. 1). The valley-filling, stratigraphically highest Rose Creek Member of the John Day Formation has also yielded fossils (Hunt and Stepleton, 2004), but so far only from paleochannels (Retallack, 2004a); thus, it is not included in the present paleosol study. In terms of North American Land Mammal 'Ages,' these members are mainly Arikareean (Figs. 2, 3), with some Whitneyan (Turtle Cove Member A) and Hemingfordian (Rose Creek Member; Tedford et al., 2004; Albright et al., 2008). The Arikareean has been divided into four parts: Ar-1 (Turtle Cove Member Units B–J), Ar-2 (Turtle Cove Member Units K1–K2), Ar-3 (Kimberly, Haystack Valley, and Balm Creek members), and Ar-4 (Johnson Canyon Member) (Albright et al., 2008). Subdivisions Ar1–Ar3 have also been called (successively) 'Geringian,' 'Monroecreekian,' and 'Harrisonian' (Alroy, 2000; Retallack, 2004a). Biostratigraphic subdivision of the John Day Formation has been based on oreodonts (Merriam and Sinclair, 1906) and rodents (Rensberger, 1971, 1973, 1983), but there is also an independent geochronology using both magnetostratigraphy (Prothero and Rensberger, 1985; Albright et al., 2008) and $^{40}Ar/^{39}Ar$
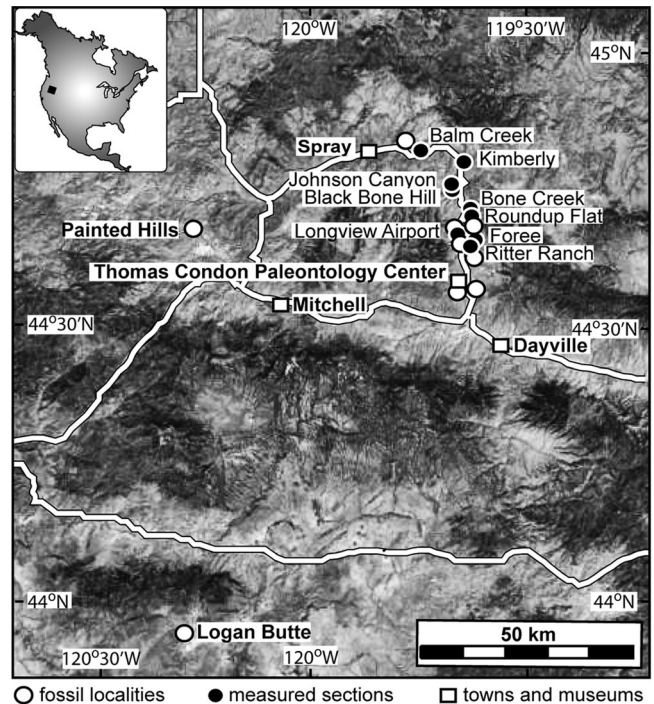

FIGURE 1. Location of geological sections examined in central Oregon. Measured sections and fossil localities were correlated using marker tuff beds (Fremd et al., 1994; Retallack et al., 2000; Hunt and Stepleton, 2004; Albright et al., 2008).

radiometrically dated tuffs (Fremd et al., 1994; Hunt and Stepleton, 2004; Retallack, 2004a; Albright et al., 2008). These dates and both magnetostratigraphic studies give very similar age models (Fig. 3). Geological age (M, in million years) can be estimated from the stratigraphic level (L, in m) using a linear fit to $^{40}Ar/^{39}Ar$ radiometric ages of tuffs (Fremd et al., 1994; Retallack, 2004a; Albright et al., 2008) for the section, as follows:

$$M = -0.0173L + 30.808 \, (n = 7; r^2 = 0.99; SE: \pm 0.46 \, Ma) \quad (1)$$

Field work for this study began in 1978, culminating in a first attempt to define paleoclimatic ranges of 238 fossils (Retallack et al., 2004). Since then, it has been refined with annual field work to inspect ongoing collections of the John Day Fossil Beds National Monument, amassing a database of 504 fossils. For each new fossil record, a field assessment was made by both authors to determine whether fossils were in place. In many cases, these were fossils excavated from within the outcrop and jacketed for transport. In other cases, they were on the surface but on erosional remnant pedestals or extensive bedding plane exposures. Other fossils found loose on the footslope or within erosional gullies were not added to our database. Most of the material was in two kinds of paleosols, the Xaxus (deep calcic) and Xaxuspa (shallow calcic) pedotypes (Figs. 4, 5), formerly Vitrand soils (glass-shard-rich Andisols). Xaxus paleosols are in repeated triplets with two overlying Xaxuspas paleosols (Fig. 4), and both have common round calcareous nodules and a distinct green color from late diagenetic celadonite (Retallack et al., 2000). Xaxus, Xaxuspa, and Micay are pedotypes based on field characteristics, but with known geochemical and petrographic character (Retallack et al., 2000). A few specimens are from weakly developed paleosols (Micay pedotype, rooted
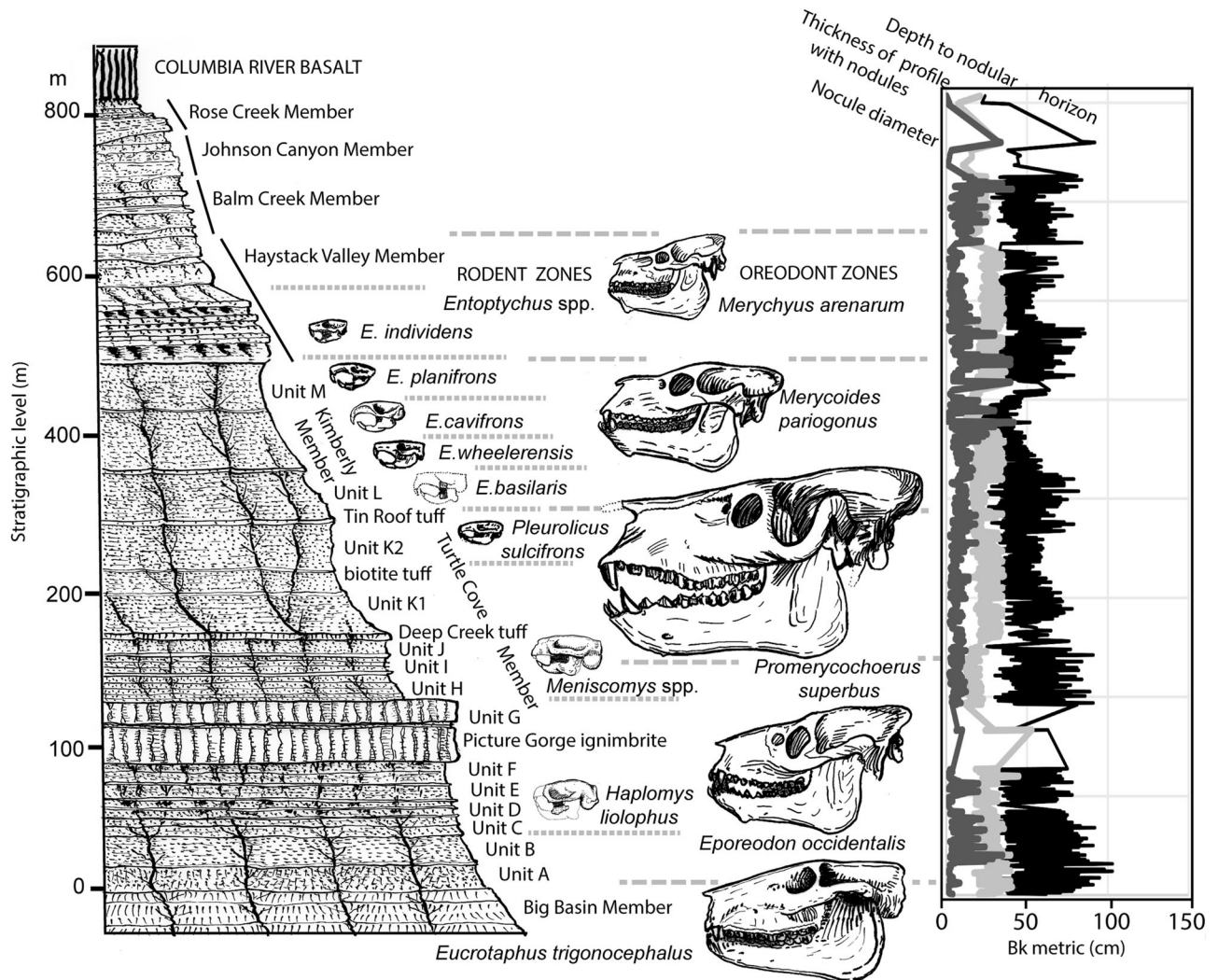
FIGURE 2. Composite section of the John Day Formation between Dayville and Spray, Oregon, with rodent and oreodont biostratigraphy, and with raw measures (all cm) of depth to calcareous nodules (light gray line), thickness of paleosols with nodules (black line), and size of calcareous nodules (dark gray line).

shale without carbonate nodules) and were entered to give stratigraphic level, but not paleoclimatic niche. Measured sections above the Picture Gorge Ignimbrite (Turtle Cove Unit G and higher) were presented by Retallack (2004a), but two new sections below the ignimbrite were measured for this study (Fig. 6) to construct a composite section of the John Day Formation above the Big Basin Member (Figs. 2, 3).

Paleosol Measurements

The primary measure taken at each fossil site was depth to calcic horizon in the paleosol (D_p, in cm), which is known in modern soils (D_s, in cm) to be related to a variety of ecological important variables: (1) mean annual precipitation (MAP; P, in mm; Retallack, 2005; Nordt et al., 2006; Beverly et al., 2018), (2) tree height (H, in m; Retallack, 2012), and (3) secondary productivity at the end of the growing season (S, in ppm CO_2; Breecker and Retallack, 2014). All three variables are related in modern ecosystems, for example, the decline in tree height in a transect from productive, humid forest of Sydney to low-productivity, arid shrublands near Broken Hill in New South Wales, Australia (Retallack, 2012). The shallow-calcic paleosols are not erosionally truncated deep-calcic paleosols, because they have root traces converging near the surface, and distinctive arid-land trace fossils (Retallack et al., 2000). Furthermore, the rate of sediment accumulation within the Turtle Cove Formation is exceptionally high for North America, allowing preservation of temporal resolution better than Milankovitch obliquity cycles (Retallack, 2007a). The relationships for mean annual precipitation are based on global data sets (Retallack, 2005; Breecker and Retallack, 2014), but the relationship for tree height is based on African trees (vegetation taller than 1.5 m in data of Retallack, 2012). The relationship between depth to calcic horizon and tree height is known to have been different for pteridophytic trees of the Devonian (Retallack and Huang, 2011) and also for Australian mallee eucalypts (Retallack, 2012). The original soil depth (D_s) can be calculated from paleosol depth (D_p) using a compaction curve for calcareous paleosols (Equation 5) for the known depth of burial (K, in km; Sheldon and Retallack, 2001), taken as 1.3 km for the John Day Valley (Retallack, 2007a). Thus, several ecological parameters, each related to productivity, can be calculated from depth to calcic horizon for each fossil,
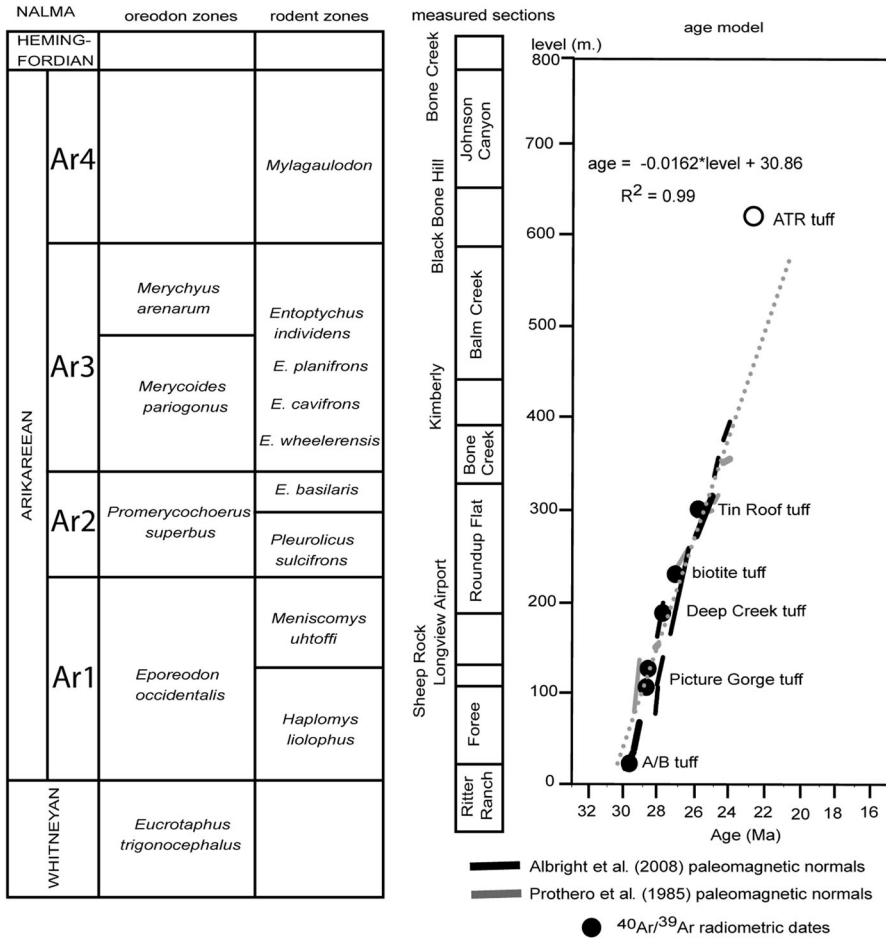
FIGURE 3. Biozones and age model for a composite section of the John Day Formation between Dayville and Spray, Oregon. The age model is based on $^{40}Ar/^{39}Ar$ dating of marker tuffs (Fremd et al., 1994; Retallack et al., 2000; Hunt and Stepleton, 2004; Albright et al., 2008), but the age of the ATR tuff is suspect and under reexamination.

using the following equations:

$$P = 137.24 + 6.45D_s$$
$$+ 0.013D_s^2 \ (n = 675; r^2 = 0.52; SE: \pm 147 \text{ mm}) \quad (2)$$

$$H = 0.2398D_s - 7.9905 \ (n = 10; r^2 = 0.88; SE: \pm 4.8 \text{ m}) \quad (3)$$

$$S = 35.4D_s + 588 \ (n = 15; r^2 = 0.54; SE: \pm 766 \text{ ppm } CO_2) \quad (4)$$

$$D_s = D_p/[-0.62/(e^{0.17K} - 1)]^{0.38} \ (\text{model without SE}) \quad (5)$$

Also measured was the thickness of paleosol with carbonate nodules (T_p, in cm) because thickness of soil with nodules (T_s, in cm) has been shown to be related to mean annual range of precipitation (MARP; R, in mm), defined as the difference between mean precipitation of the wettest month and mean precipitation of the driest month (Retallack, 2005). This measured thickness (T_p) can be converted to soil thickness (T_s) using Equation 5 for highly calcareous soils (Aridisols of Sheldon and Retallack, 2001), to gain an estimate of climatic rainfall seasonality for each fossil.

$$R = 0.79T_s + 13.71 \ (n = 675; r^2 = 0.58; SE: \pm 22 \text{ mm}) \quad (6)$$

Finally, the carbonate nodule diameter (N, in cm) of the paleosols was also measured as a guide to the duration of soil formation (A, in kyr), because soil nodules are known to grow in size with increased soil age (Machette, 1985). This measure of paleosol duration and thus ecosystem maturity does not require decompaction for nodules in clayey matrix (Retallack, 2005). The data set for this chronofunction is radiocarbon-dated soil carbonate of the Desert Project near Las Cruces, New Mexico (Gile et al., 1981).

$$A = 3.92N^{0.34} \ (n = 10; r^2 = 0.57; SE: \pm 1.8 \text{ kyr}) \quad (7)$$

These transfer functions are based on large databases of modern soils, so that their errors are standard deviations of those data. Standard deviations reported in Table 1 also include additional variance from the number of estimates on which they are based.

Fossil Identification

Our study includes only identifiable fossils found in situ, including plants, vertebrates, invertebrates, and trace fossils, but mainly mammals curated into the Condon Collection of the Museum of Natural and Cultural History of the University of Oregon, Eugene, Oregon, and the Thomas Condon Paleontology Center, John Day Fossil Beds National Monument, Kimberly, Oregon. For comprehensive surveys of the paleontology of the
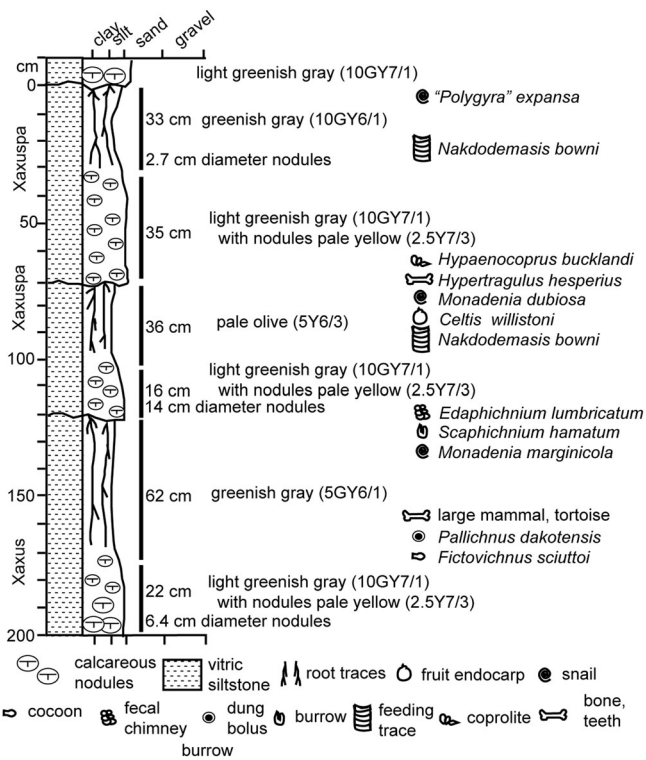
FIGURE 4. Paleosol triplet of a deep-calcic and two shallow-calcic paleosols, representing a Milankovitch obliquity (41 ka) beat, at 257–260 m in the Turtle Cove Member section of John Day Formation above the Big Basin Member.

John Day Formation, see Retallack et al. (2000), Hunt and Stepleton (2004), and Albright et al. (2008).

Only preliminary studies have yet been published of trace fossils in the John Day Formation (Retallack, 2004a), but our trace fossils are attributed to earthworms (*Edaphichnium lumbricatum* Bown and Kraus, 1983), dung beetles (*Coprinisphaera murguiai* in the extended sense of Genise, 2016; *Pallichnus dakotensis* Retallack, 1984), wasps (*Fictovichnus sciuttoi* of Genise, 2016), sweat bees (*Celliforma ficoides* Retallack, 1984), ants (small cocoons and *Socialites tumulus* Roberts and Tapanila, 2006), and termites (*Microfavichnus alveolatus* Duringer et al., 2007). *Naktodemasis bowni* is here attributed to cicadas, such as living *Okanagana*, because these meniscate burrows are identical to cicada burrows in comparable calcareous modern soils and Pleistocene paleosols of the Palouse Loess of Washington (O'Geen and Busacca, 2001), although the same general form of burrow can be made by bugs and beetles (Smith et al., 2008). The makers of *Scaphichnium hamatum* and *Macanopsis astreptum* are uncertain: perhaps spiders, wasps, beetles, cicadas, or decapods (Bown and Kraus, 1983). *Fictovichnus sciuttoi* as revised by Genise (2016) may be cocoons of a beetle or wasp. *Gyrolithes* is a narrow, loosely sinuous burrow that may have been made by scorpions, amphisbaenid lizards, or small rodents (Bown and Kraus, 1983).

The only fossil plant common in the middle and upper John Day Formation is the calcite-silica endocarps of hackberry, *Celtis willistonii* Chaney (1925). Also in the collection are fragments of wood with vessels attributed to Dicotyledonae incertae sedis. A small unpublished flora from tuffs of the lower Haystack Valley Member on Heath Ranch includes *Ulmus*, *Quercus*, Fabaceae, and Aceraceae (JODA 11013-5), and similar small-leaved dicot floras have been found elsewhere in Oligocene rocks of the western U.S.A. (Wing, 1987, 1998). Phytoliths of the John Day Formation are currently under study by C. A. Strömberg and include a mix of grasses and trees (Dillhoff et al., 2009). Oligocene pollen assemblages from western North America include saltbush (*Sarcobatu*s), a common component of modern sagebrush communities (Leopold and Denton, 1987; Leopold et al., 1992). This vegetation predates the evolutionary appearance of sod grasslands and crown-group grass phytoliths (MacFadden and Hulbert, 1988; MacFadden, 2000; Retallack, 2004c, 2007b, 2013a; Strömberg, 2011)

Fossil snail species from the John Day Formation described by Hanna (1920, 1922) were partly revised by Roth (1986) and Pierce (1992). The following sources were used for our identifications of vertebrates: rhineurids (Berman, 1976), primates (Samuels et al., 2015), rodents (Rensberger, 1971, 1973, 1983; Korth and Samuels, 2015), nimravids (Barrett, 2016), canids (Wang, 1994; Wang et al., 1999), amphicyonids (Hunt, 1998, 2009), camels (Prothero, 1996; Honey et al., 1998), entelodonts (Foss, 2007), tayassuids (Prothero, 2009, 2015), and leptochoerids (MacDonald, 1955; Theodor et al., 2007). Tortoises of the John Day Formation have not been revised since Hay (1908) and were recognized from partial carapaces, which come in thick- (>8 mm) and thin- (<8 mm) shell varieties. A small skull currently under study is a new genus of musteloid carnivore, now known as *Corumictis wolsani* (Paterson et al., 2020).

Oreodonts of the John Day Formation have been revised in an unpublished dissertation of Emery (2016), and we followed her concept of wide intraspecific variation in *Eporeodon occidentalis*. Nevertheless, we follow Lander (1998) in maintaining separation of *Eucrotaphus trigonocephalus*, which we found only in the Whitneyan Big Basin Member, well below the Arikareean first appearance of *Eporeodon occidentalis*. Additional oreodonts from the John Day Formation include the agriochoerid *Agriochoerus antiquus* and the merycoidodontids *Hypsiops johndayensis*, *Merychyus arenarum*, *Merycoides pariogonus*, *Oreodontoides oregonensis*, *Paroreodon marshi*, and *Promerycochoerus superbus* (Lander, 1998).

The John Day Formation has two recognized horse species, *Miohippus annectens* and *Mesohippus*, sp. indet., and two species of rhino, *Diceratherium armatum* and *D. annectens* (Prothero, 1998; Famoso, 2017a). The two rhino species differ mainly in size, but variation is consistently greater than sexual dimorphism at many localities in the western U.S.A. (Prothero and Rasmussen, 2008). *Mesohippus* is a small, three-toed horse, perhaps represented in our collection by unidentifiable equid remains, but all of our larger *Miohippus* limbs and jaws were assigned to *M. annectens* (MacFadden, 1998; Famoso, 2017b).

Coprolites (e.g. UOMNH121776) from the John Day Formation have not yet been systematically studied, but they appear to be mainly those of carnivorans. Many of our coprolites are similar to those of dogs and are referred to *Hyaenocoprus bucklandi* Hunt et al. (2012a). Coiled coprolites (UOMNH118103) are similar to *Strabelocoprus* Hunt et al. (2012a) but lack the elongate base of the type and only species *S. pollardi*. Also found were splattered remains referred to *Conchobromus kinneyensis* Hunt et al. (2012b), which may be a degraded coprolite but is more likely a bird or mammal regurgitate (UOMNH119033).

Astronomical Cyclostratigraphy

Spectral analysis of depth to calcic horizon, and of pedogenic carbonate stable isotopic composition (both $\delta^{18}O$ and $\delta^{13}C$), for the sequence above the Picture Gorge ignimbrite showed significant spectral power in the 41, 100, and 400 ka periods, except during a low-amplitude interval between 27.5 and 26.7 Ma (Wynn et al., 2002). Aberrations in the record occur sporadically, particularly prior to 28 Ma, and appear as single-paleosol isotopic

FIGURE 5. Milankovitch beats (obliquity cycles) marked on section of Turtle Cove Formation on Roundup Flat, Longview Ranch. **A**, stratigraphic section with labeled tuff layers. **B**, Deep Creek Tuff with a sequence of underlying beats labeled. This is only the base of the composite section (Fig. 2); others were published by Retallack (2004a).

excursions of up to 5‰ (negative). The major isotopic shift in the $\delta^{18}O$ record occurs rapidly at 25.5 Ma, mean value from about −14‰ to −12‰ (Retallack et al., 2004). Paleosols in the John Day Formation are similar to Pleistocene sequences of calcareous nodular paleosols in the Palouse Loess of Washington and Oregon in repeated triplets (Retallack et al., 2004). Each triplet

beat has a basal deep-calcic paleosol and two shallow-calcic paleosols (Fig. 4), and all three correspond to 41 kyr from the radiometrically determined age model (Fig. 3). The break in slope from the deep-calcic paleosol is a striking visual feature and is often marked by a thin calcareous bench (Fig. 5). This laterally continuous line of nodules and beds contrasts with the
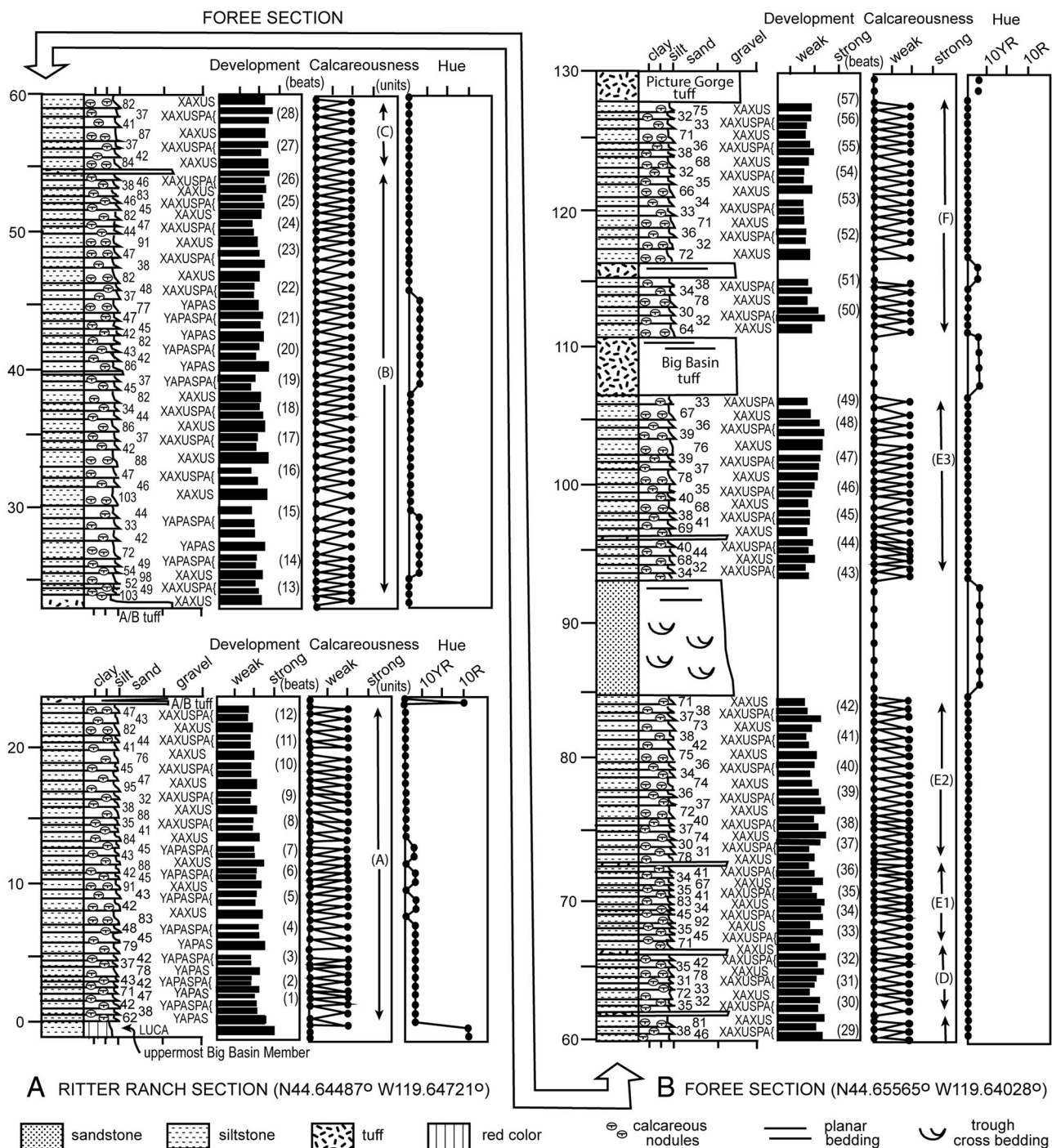
FIGURE 6. Measured sections of paleosols in the lower Turtle Cove Member strata near Ritter Ranch (**A**) and at Foree (**B**). Small numbers next to the sections are depth to calcic horizon in cm measured in the field. These sections of the lower Turtle Cove member have been combined with other sections (Retallack, 2004a) to make a composite section (Fig. 2).

nodular appearance of the rest of the slope and constitutes the base of a paleosol triplet, or Milankovitch obliquity beat. Also invaluable for correlation throughout the outcrop are the various volcanic ashes, which represent geologically instantaneous events, likely on the order of days. Thus, the stratigraphic level of any fossil can be recorded in the field as the number of beats above or below a marker ash, and then whether it is shallow or deep calcic, and whether it is the upper or lower

calcic paleosol. This level can then be read off the master sections to get a fractional meter level (fig. 6 and others of Retallack, 2004a).

A resolution of 3 paleosols per Milankovitch obliquity beat is unusual, but not exceptional. The Siwalik Group of Pakistan may have as many as 18, mostly very weakly developed paleosols per Milankovitch obliquity beat (Retallack, 1991). The Cenozoic paleosol record of Montana is comparable to the 3-paleosol-per-

TABLE 1. Precipitation, productivity, seasonality, and soil duration for each fossil taxon.

Taxon	n	Geological age (Ma)	MAP (mm) Mean ± SD	Soil CO_2 (ppm) Mean ± SD	MARP (mm) Mean ± SD	Soil age (ka) Mean ± SD	Tree height (m) Mean ± SD
Celtis willistoni	18	30.7–19.4	627 ± 215	2,713 ± 823	32 ± 4	8.3 ± 1.6	6.4 ± 5.6
Dicotyledonae	1	38.3	822	3,572	35	6.3	12.3
Rhiostoma americana	1	30.8	1,047	4,425	43	10.9	18.0
"*Polygyra*" *expansa*	19	28.5–25.4	461 ± 48	2,134 ± 209	32 ± 2	8.0 ± 1.3	2.5 ± 1.4
Vespericola dalli	28	28.4–25.0	837 ± 89	3,570 ± 320	32 ± 5	8.5 ± 0.5	12.3 ± 2.2
Monadenia dubiosa	10	28.4–24.8	461 ± 55	2,137 ± 239	31 ± 4	8.8 ± 1.3	2.5 ± 1.6
Monadenia marginicola	15	28.4–24.7	896 ± 157	3,777 ± 529	33 ± 4	7.8 ± 1.3	13.7 ± 3.6
Pallichnus dakotensis	41	30.7–25.3	840 ± 147	3,603 ± 510	34 ± 5	8.8 ± 1.5	12.5 ± 3.5
Edaphichnium lumbricatum	10	30.6–25.3	832 ± 84	3,596 ± 322	38 ± 7	7.5 ± 1.8	12.4 ± 2.2
Naktodemasis bowni	50	30.5–19.7	452 ± 67	2,234 ± 326	35 ± 6	9.0 ± 2.0	3.2 ± 2.2
Formicidae cocoons	1	29.5	440	2,066	39	6.3	2.0
Celliforma ficoides	2	28.5–25.3	914 ± 100	3,862 ± 402	40 ± 4	9.0 ± 2.0	14.2 ± 2.7
Microfavichnus alveolatus	9	28.4–25.5	846 ± 297	3,681 ± 1030	35 ± 6	8.3 ± 0.8	12.3 ± 7.0
Scaphichnium hamatum	4	28.4–26.4	714 ± 218	3,121 ± 842	34 ± 3	8.7 ± 1.0	9.2 ± 5.7
Fictovichnus sciuttoi	7	28.4–22.3	706 ± 196	3,064 ± 767	35 ± 4	8.2 ± 1.2	8.8 ± 5.2
Socialites tumulus	1	28.4	856	3,695	36	9.1	13.1
Macanopsis astreptum	1	28.2	822	3,570	36	7.9	12.2
Coprinisphaera murguiai	1	26.7	825	3,513	27	8.3	11.9
Dyticonastis rensbergeri	1	29.6	440	2,067	30	8.3	2.1
Gyrolithes	1	29.5	440	2,066	32	7.6	2.1
Stylemys (thick shell)	11	29.9–25.5	914 ± 117	3,892 ± 414	33 ± 5	8.5 ± 1.5	14.5 ± 2.8
Stylemys (thin shell)	8	28.4–25.7	587 ± 143	2,640 ± 562	33 ± 4	8.8 ± 1.1	5.9 ± 3.8
Ekgmowechashala zancanellai	2	28.2–28.0	778 ± 31	3,406 ± 117	32 ± 2	7.9 ± 1.7	11.1 ± 0.8
Haplomys liolophus	6	30.2–29.5	488 ± 83	2,273 ± 361	36 ± 8	8.2 ± 1.8	3.5 ± 2.4
Meniscomys hippodus	3	28.4–26.4	479 ± 60	2,216 ± 260	34 ± 9	8.4 ± 0.7	3.1 ± 1.8
Meniscomys uhtoffi	4	28.6–27.7	968 ± 37	4,082 ± 86	34 ± 2	7.6 ± 1.8	15.7 ± 0.9
Allotypomys pictus	1	30.1	n.a.	n.a.	n.a.	n.a.	n.a.
Palaeocastor peninsulatus	4	29.0–26.4	522 ± 50	2,407 ± 220	32 ± 3	8.4 ± 1.3	4.4 ± 1.5
Proapeomys condoni	2	29.6–29.7	1,113	4,614	28	8.6	19.4
Miosciurus ballovianus	2	27.9–26.4	729 ± 381	3,155 ± 1,450	37 ± 10	7.4 ± 0.3	9.4 ± 9.6
Protosciurus mengi	1	27.8	945	4,035	27	3.9	15.4
Leidymys nematodon	4	28.8–24.8	693 ± 247	3,044 ± 959	31 ± 6	7.6 ± 1.3	8.7 ± 6.5
Paciculus insolitus	1	25.1	460	2,122	31	8.6	2.4
Entoptychus basilaris	5	26.9–24.1	538 ± 130	2,430 ± 499	33 ± 4	9.4 ± 1.0	4.5 ± 3.4
Entoptychus cavifrons	1	25.1	809	3,454	33	9.4	11.5
Entoptychus individens	1	23.2	367	1,710	27	8.6	0
Entoptychus planifrons	2	24.2	485 ± 20	2,217 ± 85	34 ± 3	10.0 ± 0.3	3.1 ± 0.6
Entoptychus wheelerensis	2	26.7–25.0	436 ± 20	2,025 ± 93	31 ± 1	9.5 ± 0.5	1.8 ± 0.6
Pleurolicus sulcifrons	7	27.0–25.0	505 ± 108	2,307 ± 431	36 ± 5	8.6 ± 1.1	3.7 ± 2.9
Archaeolagus ennisianus	18	29.6–25.4	541 ± 135	2,460 ± 526	34 ± 5	8.3 ± 0.6	4.7 ± 3.6
Diceratherium annectens	19	30.3–25.0	896 ± 186	3,817 ± 638	37 ± 6	8.6 ± 1.7	13.9 ± 4.3
Diceratherium armatum	8	30.3–25.6	1,056 ± 261	4,364 ± 904	44 ± 4	7.9 ± 2.0	17.7 ± 6.1
Miohippus annectens	19	30.1–23.9	703 ± 164	3,110 ± 634	36 ± 10	8.2 ± 0.8	9.1 ± 4.3
Leptochoerus elegans	1	30.7	1059	4,466	42	7.6	18.4
Archaeotherium caninus	2	29.9–30.0	1,170 ± 320	4,783 ± 1,047	47 ± 1	8.8 ± 0.4	20.5 ± 7.1
Perchoerus probus	1	24.8	742	3,208	29	8.6	9.8
Marshochoerus socialis	1	22.6	819	3,423	36	8.6	11.3
Hypertragulus hesperius	31	30.7–24.0	489 ± 79	2,260 ± 333	34 ± 6	8.6 ± 1.6	3.4 ± 2.3
Hypertragulus minutus	1	29.4	458	2,148	34	7.9	2.6
Nanotragulus planiceps	7	29.5–27.7	989 ± 140	4,153 ± 481	36 ± 4	7.0 ± 1.2	16.2 ± 3.3
Gentilicamelus sternbergi	2	29.9–20.3	497 ± 68	2,258 ± 211	39 ± 17	8.2 ± 3.6	3.4 ± 1.4
Agriochoerus antiquus	5	30.1–29.6	940 ± 18	4,027 ± 64	37 ± 1	8.0 ± 0.5	15.4 ± 0.4
Eporeodon occidentalis	32	30.3–26.4	807 ± 166	3,515 ± 605	37 ± 6	8.6 ± 1.7	11.9 ± 4.1
Eucrotaphus trigonocephalus	2	30.8–30.7	1,017 ± 42	4,322 ± 146	42 ± 0	9.9 ± 1.4	14.4 ± 1.0
Hypsiops johndayensis	1	28.0	999	4,181	30	7.2	16.4
Merychyus arenarum	1	22.6	772	3,265	39	9.1	10.2
Merycoides pariogonus	3	25.4–24.7	793 ± 150	3,387 ± 546	33 ± 8	8.6 ± 0.3	11.0 ± 3.7
Paroreodon parvus	3	30.1–28.3	497 ± 68	2,308 ± 284	30 ± 5	7.4 ± 1.6	3.7 ± 1.9
Promerycochoerus superbus	7	28.1–25.3	873 ± 107	3,689 ± 375	29 ± 3	8.5 ± 0.8	13.1 ± 2.5
Cormocyon copei	1	28.0	927	3,935	32	8.6	14.7
Cynarctoides lemur	2	29.8–29.1	989 ± 396	4,139 ± 1,358	33 ± 10	8.4 ± 1.1	16.1 ± 9.2
Enhydrocyon stenocephalus	1	24.7	358	1,676	25	7.9	0
Mesocyon coryphaeus	3	29.8–26.3	719 ± 368	3,147 ± 1,439	45 ± 2	8.4 ± 1.1	9.4 ± 9.8
Paraenhydrocyon josephi	1	25.4	855	3,618	36	9.8	12.6
Phlaocyon latidens	3	29.8–28.7	692 ± 283	3,048 ± 1,140	34 ± 4	8.2 ± 0.6	8.7 ± 7.7
Rhizocyon oregonensis	2	30.0–28.2	459	2,141	31	8.9	2.6
Temnocyon altigenis	1	29.7	818	3,588	42	6.8	12.3
Hoplophoneus cerebralis	1	26.1	619	2,776	29	8.6	6.9
Nimravus brachyops	2	28.0–25.1	945 ± 76	3,959 ± 314	38 ± 11	8.3 ± 1.5	14.9 ± 2.1
Pogonodon platycopis	1	29.7	785	3,464	52	8.6	11.5
Musteloidea incertae sedis	1	25.2	763	3,293	27	9.1	10.4
Conchobromus kinneyensis	1	28.2	822	3,116	35	6.2	12.3
Hyaenacoprus bucklandensis	6	28.4–25.2	715 ± 226	3,116 ± 886	33 ± 6	8.1 ± 1.7	9.2 ± 6.0
Strabelocoprus	1	28.3	822	3,116	35	6.2	12.3

beat record in Oregon, but the thinner sequence of Badlands National Park, South Dakota, has only 1 paleosol per beat (Retallack, 1983, 1998, 2007a). Cenozoic sequences of Pakistan, Oregon, and Montana have outstanding temporal resolution because of synvolcanic and synorogenic deposition (Retallack, 2007a).

BIOSTRATIGRAPHIC RESULTS

Measurements of depth to calcareous nodules, thickness of paleosols with nodules, and size of calcareous nodules (Fig. 2) were used to calculate mean annual precipitation, mean annual range of precipitation, soil CO_2, soil age, and tree height for each in situ fossil specimen sampled. Mean values of these parameters for each taxon studied are reported in Table 1. Stratigraphic ranges of in situ specimens of the 74 taxa studied here are also in Table 1 and included in Figure 7. This improved stratigraphic acuity enables calculation of confidence intervals for first appearances following the method of Marshall (1990, 1997). For example, the first appearance of 32 samples of *Eporeodon occidentalis* is at 31.5 ± 22.8 m or 30.3 ± 0.5 Ma in the age model (Equation 1). Age uncertainty is the standard error of model fit only (Fig. 3), because the stratigraphic uncertainty is only about 0.1 m. Other oreodont first appearances are less accurately determined: first of seven *Promerycochoerus superbus* at 159 ± 103 m or 28.1 ± 3.1 Ma, and first of three *Merycoides pariogonus* at 313.0 ± 128 m and 25.4 ± 0.7 Ma. The single occurrence of *Merychus arenarum* at 472.7 m and 22.6 Ma cannot be used to define first appearance confidence intervals. This first attempt at quantitative mammalian biostratigraphy of the main oreodont zonal markers falls short of ultimate desired accuracy, but improvements will require additional specimens collected with close attention to meter level in sections.

PALEOECOLOGICAL RESULTS

Frequencies of specimens found in paleosols with varying depth to calcic (nodular) horizon are illustrated in Figures 8–11. These depths facilitate interpretation of paleoenvironmental preferences among taxa and assessment of whether certain organisms are characteristic of certain conditions.

Two distinct communities are evident from the distribution of fossils in the John Day Formation, which correspond with the shallow-calcic (Xaxuspa and Yapaspa) and deep-calcic (Xaxus and Yapas) paleosols and alternate in sequence with Milankovitch obliquity cycles (Retallack et al., 2004). The exact botanical composition of these communities is uncertain but is inferred to have been a mix of grasses and small-leaved deciduous dicots (Dillhoff et al., 2009), including hackberry (*Celtis willistoni*; Fig. 8C). The overall structure of the vegetation can be inferred from paleosol depths, which show a shallow-calcic mean of 39 ± 6 cm and a deep-calcic mean of 78 ± 12 cm (1 standard deviation). When decompacted (Equation 5), these yield tree heights of 3.0 ± 1.8 m for Xaxuspa and Yapaspa paleosols and 13.8 ± 3.4 m for Xaxus and Yapas paleosols (Equation 3). The latter (deep calcic) tree height is characteristic of a subhumid woodland, whereas the former (shallow calcic) is typical of tall shrublands such as Australian mallee. Mallee is an endemic eucalypt vegetation and also the name of several of its tree species, but extinct North American semiarid tall shrublands with legumes, walnuts, birches, and hackberries have been called cunhaka (Retallack, 2012). Trace fossils of sweat bees (*Celliforma ficoides*), ants (*Socialites tumulus*), and termites (*Microfavichnus alveolatus*) (Fig. 8D) are evidence of open patches with bare soil in this shrubland vegetation, and grass phytoliths and granular soil structure are similar to those of wooded grassland soils with bunch grasses (Retallack, 2004a).

Climatic ranges are also evident from these paleosols, with mean annual precipitation levels of 879 ± 141 mm for the subhumid woodlands and only 471 ± 59 mm for the semiarid shrublands (using Equation 2, compaction corrected with Equation 5; error here and below from values rather than transfer function standard error). This corresponds with greater secondary soil productivity for the woodlands of $3,747 \pm 497$ ppm soil CO_2, versus $2,177 \pm 254$ ppm soil CO_2 for the shrublands (from Equation 4). Mean annual range of precipitation (from Equation 6) for woodlands at 35 ± 6 mm was not different than that for shrublands at 33 ± 5 mm. Nor was estimated time of formation of paleosols (from Equation 7) in woodlands at 8.3 ± 1.4 kyr different from that in shrublands at 8.7 ± 1.3 kyr. Both shrubland and woodland paleosols represent mature, and not early successional, communities.

Even with only one or two occurrences, individual taxa of fossils in the John Day Formation can be referred to these shrubland or woodland communities, but in some cases fossils are sufficiently abundant to define their own climatic ranges (Table 1). For example, the semiarid shrubland community includes single occurrences of ant (Formicidae) cocoons (Fig. 8E), helical burrows (*Gyrolithes*; Fig. 8E), legless lizard (*Dyticonastis rensbergeri*; Fig. 9A), packrat-like cricetid (*Paciculus insolitus*; Fig. 9D), entoptychine gopher (*Entoptychus individens*; Fig. 9E), small hypertragulid (*Hypertragulus minutus*; Fig. 10C), and hesperocyonine dog (*Enhydrocyon stenocephalus*; Fig. 11B). The subhumid woodland community includes single occurrences of snail (*Rhiostoma americana*; Fig. 8A), ant nest (*Socialites tumulus*; Fig. 8D), dung beetle bolus (*Coprinisphaera murguai*; Fig. 8E), insect or spider burrow (*Macanopsis astreptum*; Fig. 8E), eomyid rodent (*Proapeomys condoni*; Fig. 9C), gopher (*Entoptychus cavifrons*; Fig. 9E), tree squirrel (*Protosciurus mengi*; Fig. 9D), peccaries (*Perchoerus probus*; *Marshochoerus socialis*; Fig. 10B), entelodont (*Archaeotherium caninus*; Fig. 10B), leptochoerid (*Leptochoerus elegans*; Fig. 10B), oreodont (*Hypsiops johndayensis*; Fig. 10E), amphicyonid (*Temnocyon altigens*; Fig. 11A), nimravids (*Hoplophoneus cerebralis*, *Pogonodon platycopis*; Fig. 11C), borophagine and hesperocyonine dogs (*Cormocyon copei*, Fig. 11A; *Paraenhydrocyon josephi*, Fig. 11B), coiled coprolites (*Strabelocoprus*; Fig. 11D), and bird or mammal regurgitate (*Conchobromus kinneyensis*; Fig. 11D). In general, large mammals were found more often in the subhumid woodland paleosols, but small mammals in the semiarid shrubland paleosols.

The most striking differences between woodland and shrubland paleosol communities are among invertebrates, including fossil snails and invertebrate trace fossils. The likely cicada burrow *Naktodemasis bowni* is ubiquitous in semiarid shrubland paleosols in the same way that comparable burrows within Pleistocene Palouse Loess are attributed to the obligate sagebrush cicada *Okanagana* (O'Geen and Busacca, 2001). Woodland paleosols, on the other hand, have geotrupine dung beetle boli (*Pallichnus dakotensis*) and earthworm chimneys (*Edaphichnium lumbricatum*; Fig. 8F). Shrubland paleosols have the snails *Monadenia dubiosa* and '*Polygyra*' *expansa*, whereas woodland paleosols have *Vespericola dalli* and *Monadenia marginicola* (Fig. 8A, B). The shrubland snails have narrower apertures than those of woodland snails, probably to reduce water loss in the dry season (Retallack et al., 2004).

Clear preferences for woodland or shrubland are also seen in tortoises and small mammals. The thick-shelled tortoise *Stylemys* was found in subhumid woodland paleosols, but the thin-shelled *Stylemys* was found in semiarid shrubland paleosols (Fig. 9A). Their size may reflect the differing productivity and predation pressure of these ecosystems. Similarly, the smaller hypertragulid *Hypertragulus hesperius* (Jewell, 2019) was found in semiarid shrubland paleosols, but the slightly larger *Nanotragulus planiceps* was found in subhumid woodland paleosols (Fig. 10C).
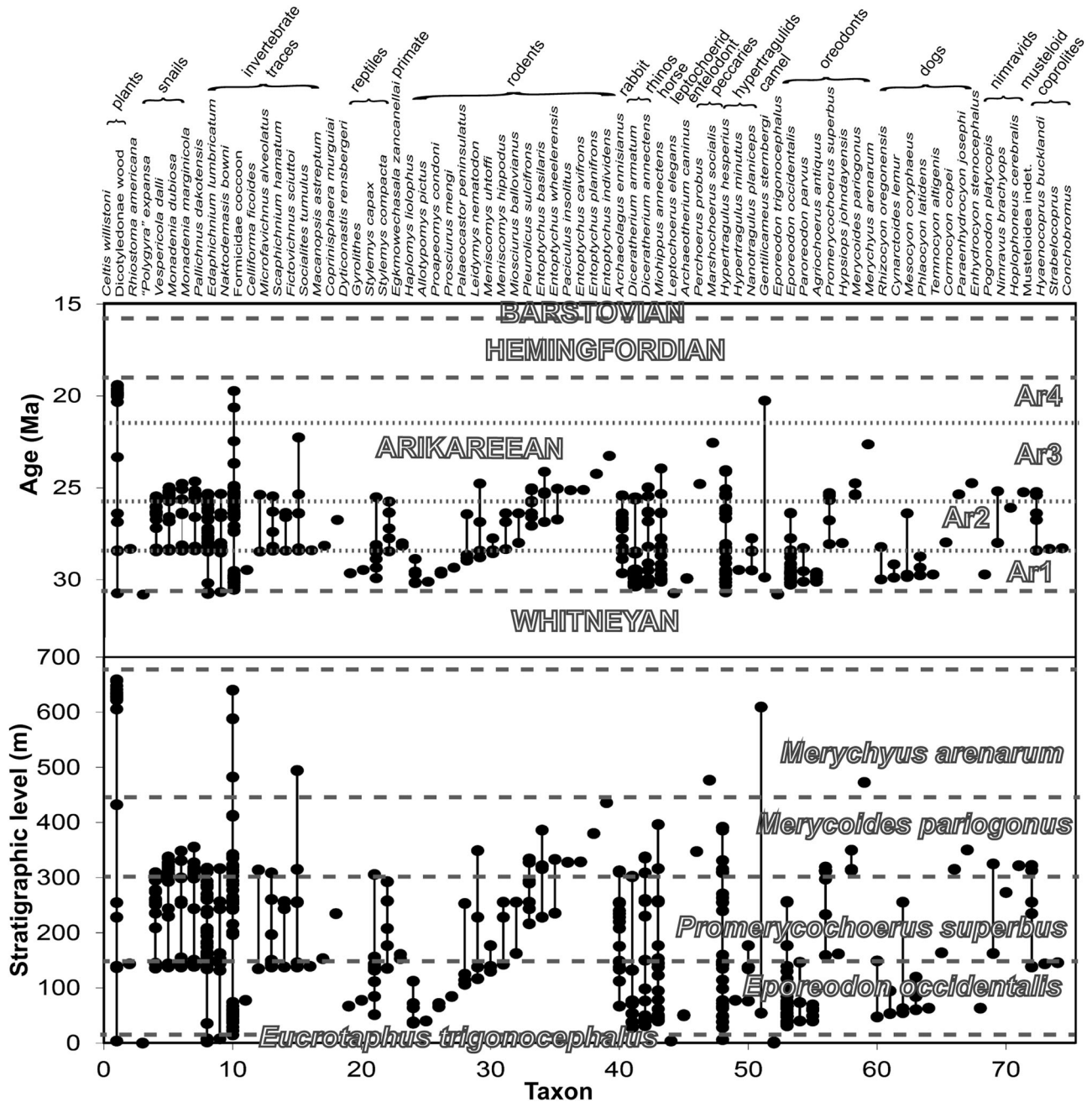
FIGURE 7. Stratigraphic ranges (with oreodont faunal zones) and estimated geological ages for 74 taxa of in situ fossils in the John Day Formation of Oregon.

Camels (*Gentilicamelus sternbergi*; Fig. 10B) were found in semi-arid shrubland paleosols, consistent with precocious cursoriality of stenomylines (Janis and Wilhelm, 1993; Janis et al., 2002).

Rodents also show clear environmental preferences and are independent evidence for open mosaic vegetation in the John Day and other Oligocene formations of North America (Samuels and Hopkins, 2017). The two species of the aplodontiid *Meniscomys* (Fig. 9B) were found in paleosols of woodlands (*M. uhtoffi*) and shrublands (*M. hippodus*), but their likely ancestor *Haplomys liolophus* was found only in shrublands (Fig. 9C). The burrowing beaver *Palaeocastor peninsulatus* also was restricted to shrublands (Fig. 9G), as expected from its cranial and postcranial morphology, which reflects fossorial habits

(Samuels and Van Valkenburgh, 2008, 2009; Calede, 2014; Korth and Samuels, 2015). Most of the geomyid gophers of the genera *Entoptychus* and *Pleurolicus* were found in semiarid shrubland soils (Fig. 9E, F). The functional morphology of *Pleurolicus* suggests that it was less exclusively fossorial than *Entoptychus* (Calede et al., 2016). Two species of generalist rodents and a rabbit straddle both shrubland and woodland communities: chipmunk-like dwarf squirrel (*Miosciurus ballovianus*; Fig. 9D), mouse-like cricetid (*Leidymys nematodon*; Fig. 9D), and archaeolagine leporid (*Archaeolagus ennisianus*; Fig. 9G).

The last known primate in North America, *Ekgmowechashala zancanellai* (Samuels et al., 2015), is represented in our data by only two records of teeth in paleosols with Bk at 67 and 71 cm,
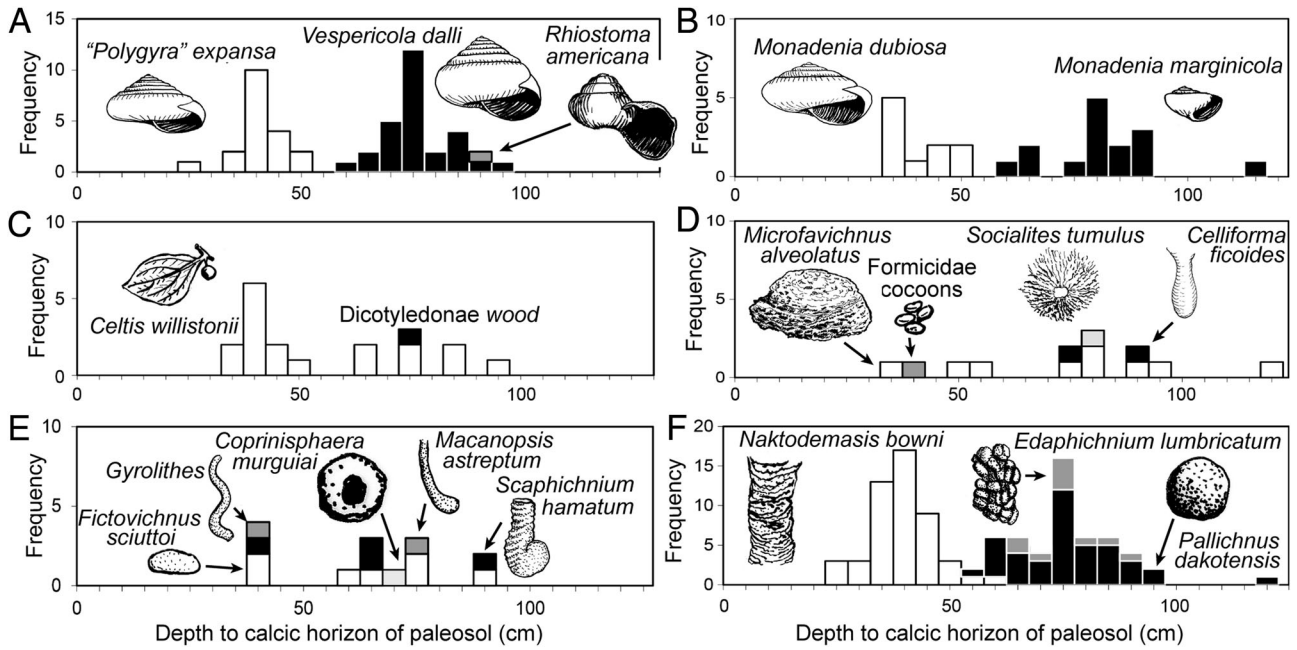
FIGURE 8. Paleoenvironmental preferences for fossil snails (**A-B**), plants (**C**), and trace fossils (**E-F**) represented as frequencies of recovered specimens arrayed on a productivity-precipitation axis from depth to calcareous nodules in their paleosol.
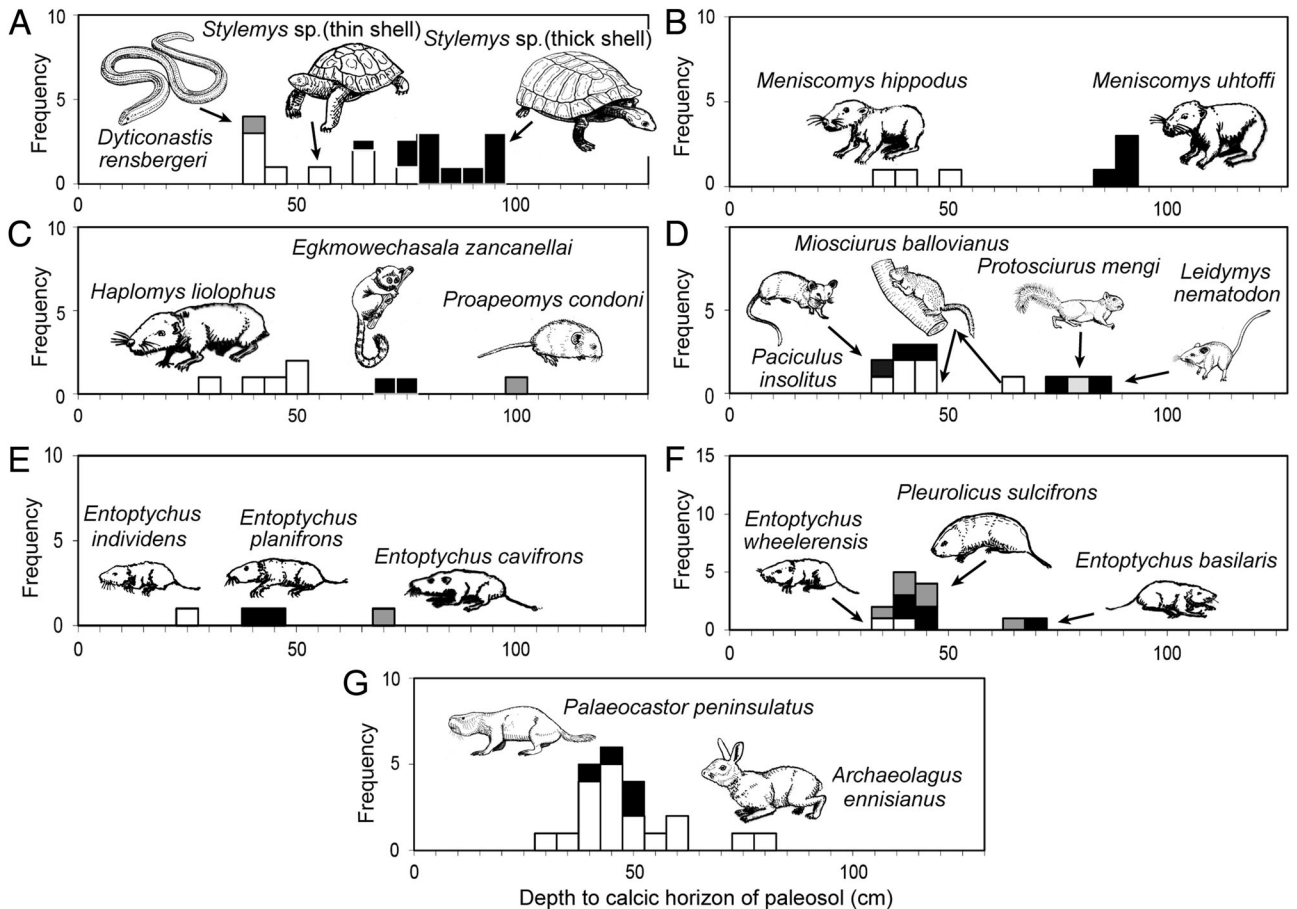

FIGURE 9. Paleoenvironmental preferences of fossil reptiles (**A**), rodents (**B-F**), rabbits (**G**), and a primate (**C**) represented as frequencies of recovered specimens arrayed on a productivity-precipitation axis from depth to calcareous nodules in their paleosol.
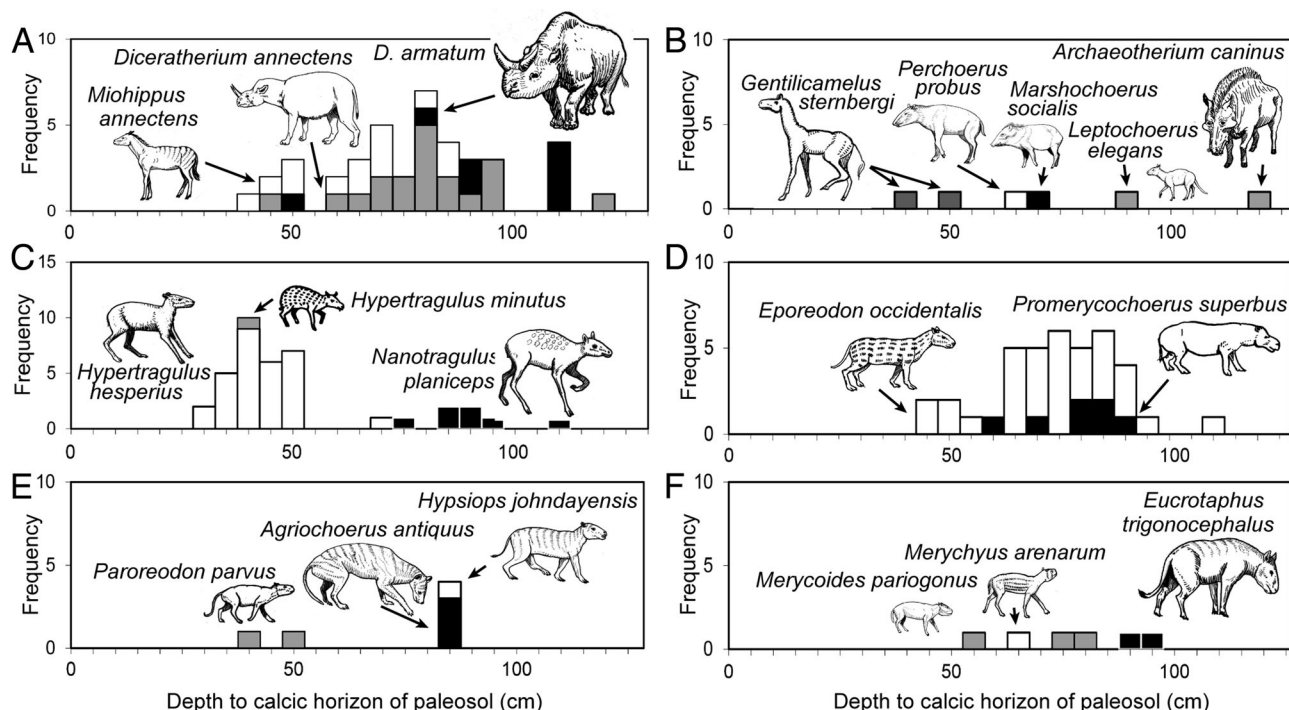
FIGURE 10. Paleoenvironmental preferences of fossil perissodatyls (**A**) and artiodactyls (**B-F**), including oreodonts (**D-F**), represented as frequencies of recovered specimens arrayed on a productivity-precipitation axis from depth to calcareous nodules in their paleosol.

corresponding to mean annual precipitation levels of 756 and 800 mm (from Equations 2 and 5) and tree heights of 10 and 12 m (from Equations 3 and 5). We envisage this creature (Fig. 9C) as arboreal in open woodland to wooded grassland, like modern African bush babies (Galagidae) (Retallack et al., 2002).

One of the horses (*Miohippus annectens*) and both rhinos (*Diceratherium annectens* and *D. armatum*) are mainly in dry woodland paleosols, but they also ventured into the wetter fringe of shrublands (Fig. 10A). This is compatible with limited mesowear and crown height of *Miohippus* (Solounias and Semprebon, 2002; Mihlbachler et al., 2011). The same pattern is seen in merycoidodontid oreodonts, especially *Eporeodon occidentalis* and *Promerycochoerus superbus*, which are represented by adequate numbers of specimens and show overlapping ranges. This is compatible with woodland habitat and C3 diet inferred from stable isotopic data for *Merycoidodon* (Zanazzi and Kohn, 2008). Persistence of the smaller *Eporeodon occidentalis* after the first appearance of the larger *Promerycochoerus superbus* (Fig. 7) may indicate some niche partitioning within the same vegetation and climate belt. The scansorial agriochoere (*Agriochoerus antiquus*) (Coombs, 1983) and other species of merycoidodontid oreodonts (*Eucrotaphus trigonocephalus*, *Paroreodon parvus*, *Hypsiops johndayensis*, *Merycoides pariogonus*, and *Merychyus arenatum*; Fig. 10E, F) are represented by few specimens but occupy comparable climatic niches to *E. occidentalis* and *P. superbus*.

Carnivorans and their likely coprolites are also represented by few specimens but show a wide climatic niche biased toward subhumid woodland paleosols such as oreodonts. Taxa straddling both semiarid shrublands and subhumid woodlands include small borophagine dog (*Phlaocyon latidens*; Fig. 11A), a hesperocyonine dog (*Mesocyon coryphaeus*; Fig. 11B), and the coprolite (*Hyaenocoprus bucklandi*; Fig. 11D). The result for *Mesocyon coryphaeus* agrees with interpretation of the species as a terrestrial mesopredator (Wang, 1994; Samuels et al., 2013) that had more generalized ecology than some other dogs and nimravids

found in the John Day Formation (Retallack, 2004b). *Phlaocyon latidens* is inferred to have been a terrestrial omnivore (Wang et al., 1999; Samuels et al., 2013), like extant raccoons, which is consistent with their occupation of a wide range of habitats. The small borophagine dog *Cynarctoides lemur* is inferred to have been a scansorial omnivore (Wang et al., 1999), like some extant procyonids, consistent with its presence in a wide climatic range in subhumid woodland paleosols (Fig. 11A). A small musteloid (Fig. 11C) and two nimravids (the incipiently cursorial *Nimravus brachyops* and robust *Pogonodon platycopis*; Fig. 11C) are in woodland paleosols, but the small scansorial sabertooth (*Hoplophoneus cerebralis*; Fig. 11C) was at the boundary between woodland and shrubland.

DISCUSSION

Ecological niches of extinct species reconstructed from the paleosols in which they are preserved have the virtue of being a proxy independent of niche inferences based on functional morphology (Kowalevsky, 1873; Rosenberger and Kinzey, 1976; Janis et al., 2002), dental microwear (Merceron et al., 2009; Mihlbachler et al., 2011), or isotopic composition (MacFadden and Higgins, 2004; Zanazzi and Kohn, 2008). Furthermore, paleosol-based niches do not assume conservation of geographic distribution or climatic niche in deep time (Waltari and Guralnick, 2009; Hadley et al., 2009; Maguire and Stigall, 2009; Nogués-Bravo, 2009; DeSantis et al., 2012).

In many instances, paleosol-based niches correspond with what would be expected for taxa based on inferences from other sources. Unsurprising distributions include the preferences of browsing oreodonts, anchitherine horses, and rhinos for woodlands over shrublands, and the preference of camels, gophers, and burrowing beavers for semiarid shrublands. Among the surprising findings is that the paleosol-based niches for some early aplodontiids suggest dry climate adaptations in early
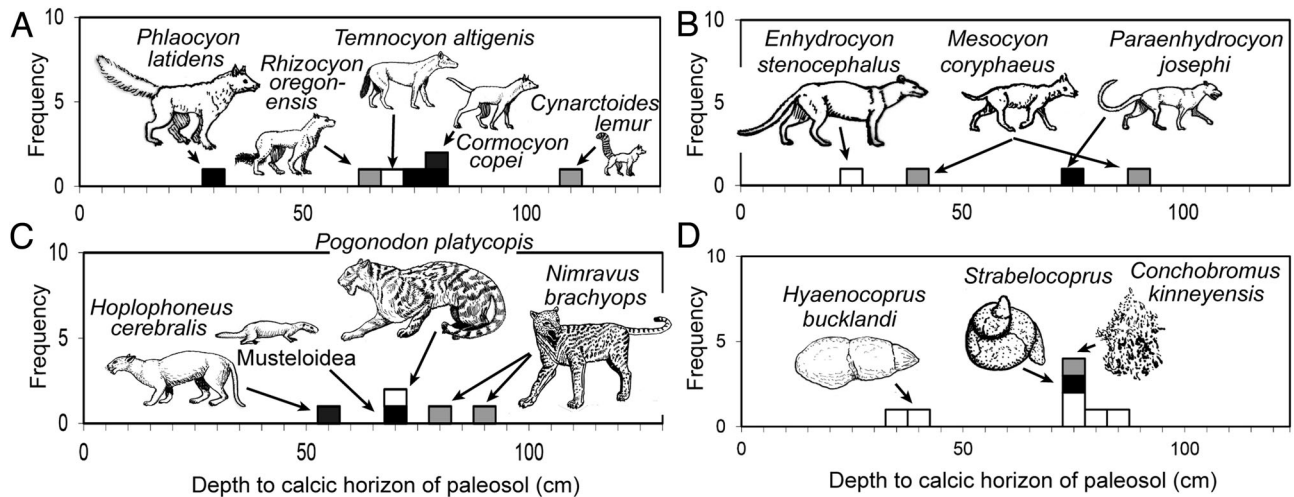
FIGURE 11. Paleoenvironmental preferences of fossil carnivorans (**A-C**) and coprolites (**D**) represented as frequencies of recovered specimens arrayed on a productivity-precipitation axis from depth to calcareous nodules in their paleosol.

representatives of a clade now found in humid climates (Hopkins, 2007). The semiarid distribution of the hypertragulid *Hypertragulus hesperius* is also a surprise, given the skeletal functional morphology comparable to modern forest tragulids (Rössner, 2007).

Although fossils of the Turtle Cove Member have been regarded as a single community evolving through several biostratigraphic zones, a pair of communities from subhumid open woodlands and semiarid shrublands are discernible from alternating shallow-calcic and deep-calcic paleosols documented here. Such paleosol alternations require very high rates of sedimentation and have been recognized rarely in vertebrate-bearing red beds: Devonian–Mississippian Catksill and Mauch Chunk formations of New York and Pennsylvania (Retallack, 2011), Permian–Triassic Archer City through Dockum formations in Texas (Retallack, 2013b), Jurassic Morrison Formation of Colorado (Retallack, 1997, 2009), and Miocene Siwalik Group of Pakistan and India (Retallack, 1991; Retallack et al., 2018). There is potential to differentiate distinct communities of vertebrates in sequences of paleosols elsewhere, after a concerted effort to improve or reevaluate collections. The recognition of these distinct communities in the Turtle Cove Member also points to past heterogeneity of habitats in the region and highlights the dynamic nature of these landscapes through time. As such, researchers should be cautious in interpreting fossil organisms recovered from these strata as actually having coexisted in the same communities, because they may instead have had different habitat preferences and were preserved in relatively close proximity as a consequence of cyclic variations in climate and the distribution of habitats.

Many other sequences are unsuitable for such studies for reasons of stratigraphic resolution and nonpedogenic facies. Quarries for vertebrate fossils in paleochannels (Lawton, 1977; Carpenter, 2013), caves (Martin and Miles, 1978; Stratford et al., 2014), or waterholes (Rogers, 1990; Mao and Retallack, 2019) lack a pedogenic overprint adequate for paleoenvironmental inferences (Retallack, 2011). There also are successions that lack paleosol alternations, such as the mammal-bearing paleosols of the Badlands of South Dakota, where there is only a single paleosol for each obliquity beat (Retallack, 1998). Both dry and humid ecosystems were melded in such paleosols, albeit overwhelmed by the contribution of the most humid and productive ecosystem, because the latter was the most significant for bioturbation. Bones from earlier millennia are less likely to be

preserved than more recent bones due to time averaging (Behrensmeyer, 1982). Preservation of communities in large collections from single Oligocene paleosols of Badlands National Park is confirmed by size distributions comparable to modern communities adjusted for known soil chemical biases (Retallack, 1988). Even in this case, niches for Oligocene mammals can be differentiated by comparing subhumid paleosols of Badlands National Park with more arid correlative paleosols deeper into the Rocky Mountain rain shadow in Nebraska and Colorado (Terry et al., 1998). Catastrophic assemblages, such as those of Ashfall Fossil Beds State Historical Park in Nebraska (Tucker et al., 2014), are also single communities that can be assessed in regional paleoclimatic gradients. Thus, depth to Bk horizon and other paleoenvironmentally significant features of paleosols can be used to assess animal niches geographically, and well in sections of unusually high temporal resolution as shown here.

Our results combine past geochronological and biostratigraphic work by Albright et al. (2008) and others with previous work on paleosols that documented cyclic oscillations in depth to Bk horizon (Retallack et al., 2004), and they also add new data on the distribution of in situ fossil specimens in John Day Formation strata. The synthesis of these methods allows the stratigraphic position of individual specimens to be tied in to levels on a composite master section (Fig. 7) and provides some biostratigraphic refinement beyond simple presence or absence in lithostratigraphic units. Because those lithostratigraphic units are often tens of meters thick in the John Day region and can span millions of years in time (Albright et al., 2008), they are not well suited for precise study and comparison of biostratigraphic distributions of taxa. The age model provided here also yields estimated geological ages for specimens (and species), resulting in greater precision than simple ranges bracketed between dated tuff layers. An additional benefit of the geological age estimates based on astronomical cyclostratigraphy is that they can be directly compared with ages derived from existing magnetostratigraphic studies (Prothero and Rensberger, 1985; Albright et al., 2008) as well as ongoing geochronological work involving Bayesian age depth modeling being pursued in the John Day region.

CONCLUSIONS

Most of the information on ancient environments used in this paper came from field observation of paleosol calcic horizons,

or Bk metrics. These include depth to the calcic horizon as a proxy for mean annual precipitation (Retallack, 2005), for tree height (Retallack, 2012), and for secondary productivity (Breecker and Retallack, 2014), and thickness of the paleosol with nodules as a proxy for mean annual range of precipitation (Retallack, 2005). The size of nodules also was measured as a proxy for time of formation and thus ecological successional maturity of the ecosystem (Retallack, 2005). Thus, precipitation, productivity, and tree height can be inferred for the habitats and niches of fossil animals found within calcareous paleosols.

Paleosols calcic horizons also show fluctuations in depth on Milankovitch obliquity (41 ka) time scales that are useful for establishing an astronomical time scale for biostratigraphy (Retallack et al., 2004). Each Milankovitch obliquity beat of 41 ka has at least three paleosols in the John Day Formation (Retallack et al., 2004). Stratigraphic level of any fossil can be recorded in the field as the number of Milankovitch obliquity beats above or below a marker ash, and then which of the three paleosols (Retallack, 2004a). This allows astronomical cyclostratigraphy to be a supplement to biostratigraphy in correlating dispersed and rare fossils to exact meter levels in a master section. Meter levels are essential to refining quantitative biostratigraphy Marshall (1990, 1997).

These preliminary results suggest that careful examination of the geological (paleopedological) context of in situ fossil specimens can provide useful information for understanding the ecology of extinct species. Unfortunately, our approach cannot be applied to most museum collections because it demands locality precision, which is unavailable. Nevertheless, our novel approach yields important ecological and biostratigraphic information on many common taxa and can be continued with future collecting. We recognize two distinct communities based on our data, with cyclic transitions between subhumid open woodlands and semiarid shrublands. These findings suggest that cyclic variations in climate drove cyclic changes in dynamic habitats and their inhabitants through time.

LITERATURE CITED

Albright, L. B., M. O. Woodburne, T. J. Fremd. C. C. Swisher, B. J. MacFadden, and G. R. Scott. 2008. Revised chronostratigraphy and biostratigraphy of the John Day Formation (Turtle Cove and Kimberly members), Oregon, with implications for updated calibration of the Arikareean North American Land Mammal Age. Journal of Geology 116:211–237.

Alroy, J. 2000. New methods for quantifying macroevolutionary patterns and processes. Paleobiology 26:707–733.

Andrews, P., J. M. Lord, and E. M. N. Evans. 1979. Patterns of ecological diversity in fossil and modern mammalian faunas. Biological Journal of the Linnean Society 11:177–205.

Barrett, P. Z. 2016. Taxonomic and systematic revisions to the North American Nimravidae (Mammalia, Carnivora). PeerJ 4:e1658.

Behrensmeyer, A. K. 1982. Time resolution in fluvial vertebrate assemblages. Paleobiology 8:211–227.

Berman, D. S. 1976. A new amphisbaenian (Reptilia: Amphisbaenia) from the Oligocene-Miocene John Day Formation, Oregon. Journal of Paleontology 50:165–174.

Beverly, E. J., W. E. Lukens, and G. E. Stinchcomb. 2018. Paleopedology as a tool for reconstructing paleoenvironments and paleoecology; pp. 151–183 in D. A. Croft, D. Su, and S. W. Simpson (eds.), Methods in Paleoecology: Reconstructing Cenozoic Terrestrial Environments and Ecological Communities, Vertebrate Paleobiology and Paleoanthropology. Springer Nature, Berlin, Germany.

Bown, T. M., and M. J. Kraus. 1983. Ichnofossils of the alluvial Willwood Formation (Lower Eocene), Bighorn Basin, northwest Wyoming, U.S.A. Palaeogeography, Palaeoclimatology, Palaeoecology 43:95–128.

Breecker, D. O., and G. J. Retallack. 2014. Refining the pedogenic carbonate atmospheric CO_2 proxy and application to Miocene CO_2. Palaeogeography, Palaeoclimatology, Palaeoecology 406:1–8.

Calede, J. J. M. 2014. Skeletal morphology of Palaeocastor peninsulatus (Rodentia, Castoridae) from the Fort Logan Formation of Montana (early Arikareean): ontogenetic and paleoecological interpretations. Journal of Mammalian Evolution 21:223–241.

Calede, J. J. M., J. X. Samuels, and M. Chen. 2016. A multi-proxy analysis of the locomotion of entoptychine gophers (Mammalia: Rodentia: Geomyidae) from the Oligocene of North America. Integrative and Comparative Biology 56:E265–E265.

Carpenter, K. 2013. History, sedimentology, and taphonomy of the Carnegie Quarry, Dinosaur National Monument, Utah. Annals of Carnegie Museum 81:153–232.

Cerling, T. E., B. H. Passey, L. K. Ayliffe, C. S. Cook, J. R. Ehleringer, J. M. Harris, M. B. Dhidha, and S. M. Kasiki. 2004. Orphans' tales: seasonal dietary changes in elephants from Tsavo National Park, Kenya. Palaeogeography, Palaeoclimatology, Palaeoecology 206:367–376.

Chaney, R. W. 1925. Notes on two fossil hackberries from the Tertiary of the Western United States. Carnegie Institution of Washington Publication 349:51–56.

Coombs, M. C. 1983. Large mammalian clawed herbivores: a comparative study. American Philosophical Society Transactions 73:1–96.

Damuth, J., and C. M. Janis. 2011. On the relationship between hypsodonty and feeding ecology in ungulate mammals, and its utility in palaeoecology. Biological Reviews 86:733–758.

Davis, E. B., J. L. McGuire, and J. D. Orcutt. 2014. Ecological niche models of mammalian glacial refugia show consistent bias. Ecography 37:1133–1138.

DeSantis, L. R., R. A. B. Tracy, C. S. Koontz, J. C. Roseberry, and M. C. Velasco. 2012. Mammalian niche conservation through deep time. PLoS ONE 7:e35624.

Dillhoff, R. M., T. A. Dillhoff, R. E. Dunn, J. A. Myers, and C. A. Strömberg. 2009. Cenozoic paleobotany of the John Day Basin, central Oregon. Geological Society of America Field Guide 15:135–164.

Duringer, P., M. Schuster, J. F. Genise, H. T. Mackaye, P. Vignaud, and M. Brunet. 2007. New termite trace fossils: galleries, nests and fungus combs from the Chad basin of Africa (Upper Miocene–Lower Pliocene). Palaeogeography, Palaeoclimatology, Palaeoecology 251:323–353.

Emery, M. 2016. Assessment of character variation in the crania and teeth of modern artiodactyls for better species diagnosis in the fossil record. Ph.D. dissertation, University of Oregon, Eugene, Oregon, 236 pp.

Famoso, N. A. 2017a. Mammalian community recovery from volcanic eruptions in the Cenozoic of North America. Ph.D. dissertation, University of Oregon, Eugene, Oregon, 112 pp.

Famoso, N. A. 2017b. Statistical analysis of dental variation in the Oligocene equid Miohippus (Mammalia, Perissodactyla) of Oregon. Journal of Paleontology 91:1060–1068.

Foss, S. E. 2007. Family Entelodontidae; pp. 120–129 in D. R. Prothero and S. E. Foss (eds.), The Evolution of Artiodactyls. Johns Hopkins University Press, Baltimore, Maryland.

Fremd, T., E. A. Bestland, and G. J. Retallack. 1994. John Day Basin Field Trip Guide and Road Log for the Society of Vertebrate Paleontology Annual Meeting. Northwest Interpretive Association, Seattle, Washington, 80 pp.

Garland, T., and C. M. Janis. 1993. Does metatarsal/femur ratio predict maximal running speed in cursorial mammals? Journal of Zoology 229:133–151.

Genise, J. F. 2016. Ichnoentomology: Insect Traces in Soils and Paleosols. Springer, Berlin, Germany, 695 pp.

Gile, L. H., J. W. Hawley, and J. B. Grossman. 1981. Soils and geomorphology in the Basin and Range area of southern New Mexico—guidebook to the Desert Project. New Mexico Bureau of Mines and Mineral Resources Memoir 39:1–222.

Hadley, E. A., P. A. Spaeth, and C. Li. 2009. Niche conservatism above the species level. Proceedings of the National Academy of Sciences of the United States of America 106:19707–19714.

Hanna, G. D. 1920. Fossil mollusks from the John Day Basin in Oregon. University of Oregon Publications 1(6):1–8.

Hanna, G. D. 1922. Freshwater mollusks from Oregon contained in the Condon Museum. University of Oregon Publications 1 (12):1–12.

Hay, O. P. 1908. The Fossil Turtles of North America. Carnegie Institution of Washington Publication 75:1–568.

Hoffman, J. M., D. Fraser, and M. T. Clementz. 2015. Controlled feeding trials with ungulates: a new application of in vivo dental molding to assess the abrasive factors of microwear. Journal of Experimental Biology 218:1538–1547.

Honey, J. G., J. A. Harrison, D. R. Prothero, and M. S. Stevens. 1998. Camelidae; pp. 439–462 in C. M. Janis, K. M. Scott, and L. L. Jacobs (eds.), Evolution of Tertiary Mammals of North America. Terrestrial Carnivores, Ungulates and Ungulatelike Mammals, Volume 1. Cambridge University Press, Cambridge, U.K.

Hopkins, S. S. 2007. Causes of lineage decline in the Aplodontidae: testing for the influence of physical and biological change. Palaeogeography, Palaeoclimatology, Palaeoecology 246:331–353.

Hunt, A. P., S. G. Lucas, and J. Spielmann. 2012a. New coprolite ichnotaxa from the Buckland Collection at Oxford University Museum of Natural History. New Mexico Museum of Natural History Bulletin 57:115–124.

Hunt, A. P., S. G. Lucas, J. A. Spielmann, A. Cantrell, T. Suazo, and A. J. Lerner. 2012b. Bromalites from the Tinajas Lagerstätte (Late Pennsylvanian: Late Missourian), central New Mexico, USA. New Mexico Museum of Natural History Science Bulletin 57:175–183.

Hunt, R. M. 1998. Amphicyonidae; pp. 196–227 in C. M. Janis, K. M. Scott, and L. L. Jacobs (eds.), Evolution of Tertiary Mammals of North America. Terrestrial Carnivores, Ungulates and Ungulatelike Mammals, Volume 1. Cambridge University Press, Cambridge, U.K.

Hunt, R. M. 2009. Long-legged pursuit carnivorans (Amphicyonidae, Daphoeninae) from the early Miocene of North America. American Museum of Natural History Bulletin 318:1–95.

Hunt, R. M., and E. Stepleton. 2004. Geology and paleontology of the upper John Day beds, John Day River Valley, Oregon: lithostratigraphic and biochronologic revision in the Haystack Valley and Kimberly areas (Kimberly and Mt. Misery quadrangles). American Museum of Natural History Bulletin 282:1–90.

Janis, C. M. 1988. An estimation of tooth volume and hypsodonty indices in ungulate mammals, and the correlation of these factors with dietary preference. Mémoires du Muséum National d'Histoire Naturelle Paris C53:367–387.

Janis, C. M., and M. Fortelius. 1988. On the means whereby mammals achieve increased functional durability of their dentitions, with special reference to limiting factors. Biological Reviews 63:197–230.

Janis, C. M., and P. B. Wilhelm. 1993. Were there mammalian pursuit predators in the Tertiary? Dances with wolf avatars. Journal of Mammalian Evolution 1:103–125.

Janis, C. M., J. Damuth, and J. M. Theodor. 2002. The origins and evolution of the North American grassland biome: the story from the hoofed mammals. Palaeogeography, Palaeoclimatology, Palaeoecology 177:183–198.

Jardine, P. E., C. M. Janis, S. Sahney, and M. J. Benton. 2012. Grit not grass: concordant patterns of early origin of hypsodonty in Great Plains ungulates and glires. Palaeogeography, Palaeoclimatology, Palaeoecology 365:1–10.

Jewell, L. K. 2019. Species diversity in the hypertragulid (Mammalia: Artiodactyla) population of the John Day Basin, Oregon. Portland State University Honors Theses 718:1–23.

Korth, W. W., and J. X. Samuels. 2015. New rodent material from the John Day Formation (Arikareean, middle Oligocene to early Miocene) of Oregon. Annals of Carnegie Museum 83:19–84.

Kowalevsky, V. 1873. Sur l'Anchitherium aurelianense Cuv., et sur l'histoire paleontologique des chevaux. Memoire Academie Imperiale des Sciences St.-Petersburg 20:1–73.

Lander, B. 1998. Oreodontoidea; pp. 402–425 in C. M. Janis, K. M. Scott, and L. L. Jacobs (eds.), Evolution of Tertiary Mammals of North America. Terrestrial Carnivores, Ungulates and Ungulatelike Mammals, Volume 1. Cambridge University Press, Cambridge, U.K.

Lawton, R. 1977. Taphonomy of the dinosaur quarry, Dinosaur National Monument. Rocky Mountain Geology 15:119–126.

Leopold, E. B., and M. F. Denton. 1987. Comparative age of grassland and steppe east and west of the Rocky Mountains. Missouri Botanical Garden Annals 74:841–867.

Leopold, E. B., G.-W. Liu, and S. Clay-Poole. 1992. Low biomass vegetation in the Oligocene?; pp. 399–420 in D. R. Prothero and W. A. Berggren (eds.), Eocene–Oligocene Climatic and Biotic Evolution. Princeton University Press, Princeton, New Jersey.

Machette, M. N. 1985. Calcic soils of the southwestern United States; pp. 10–21 in D. L. Weide (ed.), Soils and Quaternary Geology of the Southwestern United States. Geological Society of America Special Paper 203. Boulder, Colorado.

MacDonald, J. R. 1955. The Leptochoeridae. Journal of Paleontology 29:439–459.

MacFadden, B. J. 1998. Equidae; pp. 537–559 in C. M. Janis, K. M. Scott, and L. L. Jacobs (eds.), Evolution of Tertiary Mammals of North America. Terrestrial Carnivores, Ungulates and Ungulatelike Mammals, Volume 1. Cambridge University Press, Cambridge, U.K.

MacFadden, B. J. 2000. Origin and evolution of the grazing guild in Cenozoic New World mammals; pp. 223–243 in H. D. Sues (ed.), Evolution of Herbivory in Terrestrial Vertebrates: Perspectives from the Fossil Record. Cambridge University Press, Cambridge, U.K.

MacFadden, B. J., and P. Higgins. 2004. Ancient ecology of 15-million-year-old browsing mammals within C3 plant communities from Panama. Oecologia 140:169–182.

MacFadden, B. J., and R. C. Hulbert. 1988. Explosive speciation at the base of the adaptive radiation of Miocene grazing horses. Nature 336:466–468.

Maguire, K. C., and A. L. Stigall. 2009. Using ecological niche modeling for quantitative biogeographic analysis: a case study of Miocene and Pliocene Equinae in the Great Plains. Paleobiology 35:587–611.

Mao, X.-G., and G. J. Retallack. 2019. Late Miocene drying of central Australia. Palaeogeography, Palaeoclimatology, Palaeoecology 514:292–304.

Marshall, C. R. 1990. Confidence intervals on stratigraphic ranges. Paleobiology 16:1–10.

Marshall, C. R. 1997. Confidence intervals on stratigraphic ranges with nonrandom distributions of fossil horizons. Paleobiology 23:165–173.

Martin, L. D., and G. B. Miles. 1978. Excavations at Natural Trap Cave. Transactions of the Nebraska Academy of Sciences 336:107–118.

McGuire, J. L., and E. B. Davis. 2014. Conservation paleobiogeography: the past, present and future of species distributions. Ecography 37:1092–1094.

Merceron, G., J. Scott, R. S. Scott, D. Geraads, N. Spassov, and P. S. Ungar. 2009. Folivory or fruit/seed predation for Mesopithecus, an earliest colobine from the late Miocene of Eurasia? Journal of Human Evolution 57:732–738.

Merriam, J. C., and W. J. Sinclair. 1906. Tertiary faunas of the John Day region. University of California Publications in Geological Sciences 5:171–205.

Mihlbachler, M. C., F. Rivals, N. Solounias, and G. M. Semprebon. 2011. Dietary change and evolution of horses in North America. Science 331:1178–1181.

Nogués-Bravo, D. 2009. Predicting the past distribution of species climatic niches. Global Ecology and Biogeography 18:521–531.

Nordt, L., M. Orosz, S. Driese, and J. Tubbs. 2006. Vertisol carbonate properties in relation to mean annual precipitation: implications for paleoprecipitation estimates. Journal of Geology 114:501–510.

O'Geen, A. T., and A. J. Busacca. 2001. Faunal burrows as indicators of palaeovegetation in eastern Washington. Palaeogeography, Palaeoclimatology, Palaeoecology 169:23–37.

Paterson, R., Samuels, J. X., Rybczynski, N., Ryan, M. J. and Maddin, H. C. 2020. The earliest mustelid in North America. Zoological Journal of the Linnean Society 188:1318–1339.

Pierce, H. G. 1992. The non-marine molluscs of the late Oligocene–early Miocene Cabbage Patch fauna of western Montana. II. Terrestrial gastropod families other than Pupillidae (Pulmonata, Stylommatophora). Journal of Paleontology 66:610–620.

Prothero, D. R. 1996. Camelidae; pp. 609–651 in D. R. Prothero and R. J. Emry (eds.), The Terrestrial Eocene–Oligocene transition in North America. Cambridge University Press, Cambridge, U.K.

Prothero, D. R. 1998. Rhinocerotidae; pp. 595–605 in C. M. Janis, K. M. Scott, and L. L. Jacobs (eds.), Evolution of Tertiary Mammals of North America. Terrestrial Carnivores, Ungulates and Ungulatelike Mammals, Volume 1. Cambridge University Press, Cambridge, U.K.

Prothero, D. R. 2009. The early evolution of the North American peccaries (Artiodactyla: Tayassuidae): pp. 509–541 in L. B. Albright (ed.), Papers on Geology, Vertebrate Paleontology, and

Biostratigraphy in Honor of Michael O. Woodburne. Museum of Northern Arizona Bulletin 65. Flagstaff, Arizon.

Prothero, D. R. 2015. Evolution of the early Miocene hesperhine peccaries: pp. 235–256 in R. M. Sullivan and S. G. Lucas (ed.), Fossil Record 4. New Mexico Museum of Natural History and Science Bulletin 67. Albuquerque, New Mexico.

Prothero, D. R., and D. P. Rasmussen. 2008. New giant rhinoceros from the Arikareean (Oligocene-Miocene) of Montana, South Dakota and Wyoming; pp. 323–329 in S. G. Lucas, G. S. Morgan, and J. A. Spielmann (eds.), Neogene Mammals. New Mexico Museum of Natural History and Science Bulletin 44. Albuquerque, New Mexico.

Prothero, D. R., and J. M. Rensberger. 1985. Preliminary magnetostratigraphy of the John Day Formation, Oregon, and the North American Oligocene–Miocene boundary. Newsletters in Stratigraphy 15:59–70.

Rensberger, J. M. 1971. Entoptychine pocket gophers (Mammalia, Geomyoidea) of the early Miocene, John Day Formation, Oregon. University of California Publications in Geological Sciences 90:1–209.

Rensberger, J. M. 1973. Pleurolicine rodents (Geomyoidea) of the John Day Formation, Oregon. University of California Publications in Geological Sciences 102:1–95.

Rensberger, J. M. 1983. Successions of Meniscomyine and Allomyine rodents (Aplodontidae) in the Oligo–Miocene John Day Formation, Oregon. University of California Publications in Geological Sciences 124:1–157.

Retallack, G. J. 1983. Late Eocene and Oligocene Paleosols from Badlands National Park, South Dakota. Geological Society of America Special Paper 193. Boulder, Colorado, 82 pp.

Retallack, G. J. 1984. Trace fossils of burrowing beetles and bees in an Oligocene paleosol, Badlands National Park, South Dakota. Journal of Paleontology 58:571–592.

Retallack, G. J. 1988. Down to earth approaches to vertebrate paleontology. Palaios 3:335–344.

Retallack, G. J. 1991. Miocene Paleosols and Ape Habitats in Pakistan and Kenya. Oxford University Press, New York, 352 pp.

Retallack, G. J. 1997. Dinosaurs and dirt; pp. 345–359 in D. L. Wolberg, E. Stump, and G. D. Rosenberg (eds.), Dinofest International. Academy of Natural Sciences, Philadelphia, Pennsylvania.

Retallack, G. J. 1998. Fossil soils and completeness of the rock and fossil record; pp. 131–162 in S. K. Donovan and C. R. C. Paul (eds.), The Adequacy of the Fossil Record. Wiley, Chichester, U.K.

Retallack, G. J. 2004a. Late Oligocene bunch grassland and early Miocene sod grassland paleosols from central Oregon, USA. Palaeogeography, Palaeoclimatology, Palaeoecology 207:203–237.

Retallack, G. J. 2004b. Ecological polarities of Cenozoic fossil soils, plants and animals from central Oregon. Paleobiology 30:561–588.

Retallack, G. J. 2004c. Late Miocene climate and life on land in Oregon within a context of Neogene global change. Palaeogeography, Palaeclimatology, Palaeoecology 214:97–123.

Retallack, G. J. 2005. Pedogenic carbonate proxies for amount and seasonality of precipitation in paleosols. Geology 33:333–336.

Retallack, G. J. 2007a. Cenozoic paleoclimate on land in North America. Journal of Geology 115:271–194.

Retallack, G. J. 2007b. Coevolution of life and earth; pp. 295–320 in G. Schubert (ed.), Earth Evolution, Treatise of Geophysics. Elsevier, Amsterdam, The Netherlands.

Retallack, G. J. 2009. Greenhouse crises of the past 300 million years. Geological Society of America Bulletin 121:1441–1455.

Retallack, G. J. 2011. Woodland hypothesis for Devonian evolution of tetrapods. Journal of Geology 119:235–258.

Retallack, G. J. 2012. Mallee model for Mesozoic and early Cenozoic mammalian communities. Palaeogeography, Palaeoclimatology, Palaeoecology 342–343:111–129.

Retallack, G. J. 2013a. Global cooling by grasslands in the geological past and near future. Annual Reviews of Earth and Planetary Science 41:69–86.

Retallack, G. J. 2013b. Permian and Triassic greenhouse crises. Gondwana Research 24:90–103.

Retallack, G. J., and C.-M. Huang. 2011. Ecology and evolution of Devonian trees in New York, USA. Palaeogeography, Paleoclimatology, Paleoecology 299:110–128.

Retallack, G. J., E. A. Bestland, and T. J. Fremd. 2000. Eocene and Oligocene Paleosols of Central Oregon. Geological Society of America Special Paper 344. Boulder, Colorado, 192 pp.

Retallack, G. J., J. G. Wynn, and T. J. Fremd. 2004. Glacial-interglacial-scale paleoclimatic changes without large ice sheets in the Oligocene of central Oregon. Geology 32:297–300.

Retallack, G. J., J. G. Wynn, B. R. Benefit, and M. L. McCrossin. 2002. Paleosols and paleoenvironments of the middle Miocene, Maboko Formation, Kenya. Journal of Human Evolution 42:659–703.

Retallack, G. J., S. Bajpai, X. Liu, V. V. Kapur, and S. K. Pandey. 2018. Advent of strong Indian monsoon by 20 million years ago. Journal of Geology 126:1–24.

Roberts, E. M., and L. Tapanila. 2006. A new social insect nest from the Upper Cretaceous Kaiparowits Formation of southern Utah. Journal of Paleontology 80:768–774.

Rogers, R. R. 1990. Taphonomy of three dinosaur bone beds in the Upper Cretaceous Two Medicine Formation of northwestern Montana: evidence for drought-related mortality. Palaios 5:394–413.

Rosenberger, A. L., and W. G. Kinzey. 1976. Functional patterns of molar occlusion in platyrrhine primates. American Journal of Physical Anthropology 45:281–297.

Rössner, G. E. 2007. Family Tragulidae; pp. 213–220 in D. R. Prothero and S. E. Foss (eds.), The Evolution of Artiodactyls. Johns Hopkins University Press, Baltimore, Maryland.

Roth, B. 1986. Land mollusks (Gastropoda, Pulmonata) from the early Tertiary Bozeman Group, Montana. California Academy of Science Proceedings 49:237–267.

Samuels, J. X., and S. S. Hopkins. 2017. The impacts of Cenozoic climate and habitat changes on small mammal diversity of North America. Global and Planetary Change 149:36–52.

Samuels, J. X., and B. Van Valkenburgh. 2008. Skeletal indicators of locomotor adaptations in living and extinct rodents. Journal of Morphology 269:1387–1411.

Samuels, J. X., and B. Van Valkenburgh. 2009. Craniodental adaptations for digging in extinct burrowing beavers. Journal of Vertebrate Paleontology 29:254–268.

Samuels, J. X., L. B. Albright, and T. J. Fremd. 2015. The last fossil primate in North America, new material of the enigmatic *Ekgmowechashala* from the Arikareean of Oregon. American Journal of Physical Anthropology 158:43–54.

Samuels, J. X., J. A., Meachen, and S. A. Sakai. 2013. Postcranial morphology and locomotor habits of living and extinct carnivorans. Journal of Morphology 274:121–146.

Sheldon, N. D., and G. J. Retallack. 2001. Equation for compaction of paleosols due to burial. Geology 29:247–250.

Sheldon, N. D., and N. J. Tabor. 2009. Quantitative paleoenvironmental and paleoclimatic reconstruction using paleosols. Earth-Science Reviews 95:1–52.

Smith, J. J., S. T. Hasiotis, M. J. Kraus, and D. T. Woody. 2008. *Naktodemasis bowni*: new ichnogenus and ichnospecies for adhesive meniscate burrows (AMB), and paleoenvironmental implications, Paleogene Willwood Formation, Bighorn Basin, Wyoming. Journal of Paleontology 82:267–278.

Solounias, N., and G. Semprebon. 2002. Advances in the reconstruction of ungulate ecomorphology with application to early fossil equids. American Museum Novitates 3366:1–49.

Solounias, N., M. Teaford, and A. Walker. 1988. Interpreting the diet of extinct ruminants: the case of a non-browsing giraffid. Paleobiology 14:287–300.

Stirton, R. A. 1947. Observations on evolutionary rates in hypsodonty. Evolution 1:32–41.

Stratford, D., S. Grab, and T. R. Pickering. 2014. The stratigraphy and formation history of fossil-and artefact-bearing sediments in the Milner Hall, Sterkfontein Cave, South Africa: new interpretations and implications for palaeoanthropology and archaeology. Journal of African Earth Sciences 96:155–167.

Strömberg, C. A. 2011. Evolution of grasses and grassland ecosystems. Annual Review of Earth and Planetary Sciences 39:517–544.

Tedford, R. H., L. B. Albright, A. D. Barnosky, I. Ferrusquia-Villafranca, R. M. Hunt, J. E. Storer, C. C. Swisher, M. R. Voorhies, S. D. Webb, and D. P. Whistler. 2004. Mammalian biochronology of the Arikareean through Hemphillian interval (late Oligocene through early Pliocene epochs); pp. 169–231 in M. O. Woodburne (ed.), Late Cretaceous and Cenozoic Mammals of North America: Biostratigraphy and Geochronology. Columbia University Press, New York.

Terry, D. O., H. E. LaGarry, and R. M. Hunt (eds). 1998. Depositional Environments, Lithostratigraphy, and Biostratigraphy of the White River and Arikaree Groups (Late Eocene to Early Miocene, North America). Geological Society of America Special Paper 325. Boulder, Colorado, 216 pp.

Theodor, J. M., J. Erfurt, and G. Métais. 2007. The earliest artiodactyls: Diacodexidae, Dichobunidae, Homacodontidae, Leptochoeridae, and Raoellidae: pp. 32–58 in D. R. Prothero and S. E. Foss (eds.), The Evolution of Atiodactyls. Johns Hopkins University Press, Baltimore, Maryland.

Tucker, S. T., R. E. Otto, R. M. Joeckel, and M. R. Voorhies. 2014. The geology and paleontology of Ashfall Fossil Beds, a late Miocene (Clarendonian) mass-death assemblage, Antelope County and adjacent Knox County, Nebraska, USA. Geological Society of America Field Guides 36:1–22.

Van Valen, L. V. 1960. A functional index of hypsodonty. Evolution 14:531–532.

Van Valkenburgh, B. 1985. Locomotor diversity within past and present guilds of large predatory mammals. Paleobiology 11:406–428.

Waltari, E., and R. P. Guralnick. 2009. Ecological niche modelling of montane mammals in the Great Basin, North America: examining past and present connectivity of species across basins and ranges. Journal of Biogeography 36:148–161.

Wang, X. 1994. Phylogenetic systematics of the Hesperocyoninae (Carnivora, Canidae). American Museum of Natural History Bulletin 221:1–207.

Wang, X., R. H. Tedford, and B. E. Taylor. 1999. Phylogenetic systematics of the Borophaginae (Carnivora, Canidae). American Museum Natural History Bulletin 243:1–391.

Wing, S. L. 1987. Eocene and Oligocene floras and vegetation of the northern Rocky Mountains. Missouri Botanical Garden Annals 74:748–754.

Wing, S. L. 1998. Tertiary vegetation of North America as a context for mammalian evolution; pp. 37–65 in C. M. Janis, K. M. Scott, and L. L. Jacobs (eds.), Evolution of Tertiary Mammals of North America. Terrestrial Carnivores, Ungulates and Ungulatelike Mammals, Volume 1. Cambridge University Press, Cambridge, U.K.

Wynn, J. G., G. J. Retallack, and T. J. Fremd. 2002. Long-term, high-frequency terrestrial paleoclimatic record from carbon and oxygen isotopes of pedogenic carbonate from the Late Oligocene to Early Miocene John Day Formation at Longview Ranch, Central Oregon (28.7–23.6 Ma). Annual Meeting of the American Geophysical Union Abstracts (San Francisco). Eos 83 (47):F877.

Zanazzi, A., and M. J. Kohn. 2008. Ecology and physiology of White River mammals based on stable isotope ratios of teeth. Palaeogeography, Palaeoclimatology, Palaeoecology 257:22–37.